9

Review Article

Xiaoyan Liu, Yijie Wang, Yu Wang, Yize Zhao, Jinghao Yu, Xinyi Shan, Yi Tong*, Xiaojuan Lian, Xiang Wan, Lei Wang*, Pengfei Tian*, and Hao-Chung Kuo*

Recent advances in perovskites-based optoelectronics

https://doi.org/10.1515/ntrev-2022-0494 received March 19, 2022; accepted September 14, 2022

Abstract: The development and utilization of perovskites are beneficial to improve or even change the optical properties of devices and obtain fascinating performances such as higher photoelectric conversion efficiency, better thermal stability, higher external quantum efficiency, more excellent remodeling, and flexibility. So, there are many articles on perovskite reviews having been reported from synthesis, properties to various applications (such as optoelectronic devices, electrical memristor, etc.). Based on the reported review of perovskites, this study will make a further supplement to the research progress of perovskites in visible light communication (VLC), optical neuromorphic devices, and highlight huge development prospects in these emerging fields in recent years. First, we briefly reviewed the preparation methods of common perovskite materials, followed by the optical and electrical characteristics. Then, the specific applications of optical

properties based on perovskite materials are emphatically investigated, in addition to traditional photovoltaic devices. especially the latest cutting-edge fields of information encryption and decryption, VLC as well as optical memristive devices for photonic synapse and photonic neuromorphic computing. Finally, the main conclusions and prospects are given. Perovskite-based optical memristive devices are enabled to assist photonic neuromorphic calculations, showing huge potential application prospects in intelligent integrated chip fusing sensing, storage, and computing.

Keywords: perovskite materials, optical memristive devices, photonic synapse and photonic neuromorphic computing, visible light communication, information encryption and decryption

1 Introduction

As a semiconductor material and a new type of functional material with huge application potential, perovskite is developing rapidly. Perovskite refers to a class of compounds that have a chemical structure similar to calcium titanate (CaTiO₃), which was the first perovskite material discovered in 1839. Its molecular formula can be expressed as ABX₃ structure, where A, B, and X represent different elements. A represents the organic or inorganic cations, such as CH₃NH₃⁺, CH(NH₂)₂⁺, and Cs⁺, B denotes the metal ions, such as Sn^{2+} and Pb^{2+} , and X is the halogen anions such as Cl⁻, Br⁻, and I⁻ [1,2]. The crystal structure of the perovskite material has a stable and regular octahedral structure, with the metal cation B as the nucleus, the halogen anion at the top corner, and the organic or inorganic cation in the middle to balance the charge [3].

Studies have found that perovskite materials have excellent photoelectric properties, suitable band gap, strong light absorption, high luminous efficiency, strong carrier mobility, high ion conductivity, and long carrier lifetime. The distinctive photoelectric properties of perovskite materials make it have broad application prospects in

Xiaoyan Liu, Yijie Wang, Yu Wang, Yize Zhao, Jinghao Yu, Xiaojuan Lian, Xiang Wan: College of Integrated Circuit Science and Engineering, Nanjing University of Posts and Telecommunications, Nanjing, 210023, China

Xinyi Shan: School of Information Science and Technology, Fudan University, Shanghai 200433, China

^{*} Corresponding author: Yi Tong, College of Integrated Circuit Science and Engineering, Nanjing University of Posts and Telecommunications, Nanjing, 210023, China,

e-mail: tongyi@njupt.edu.cn

^{*} Corresponding author: Lei Wang, College of Integrated Circuit Science and Engineering, Nanjing University of Posts and Telecommunications, Nanjing, 210023, China,

e-mail: leiwang1980@njupt.edu.cn

^{*} Corresponding author: Pengfei Tian, School of Information Science and Technology, Fudan University, Shanghai 200433, China, e-mail: pftian@fudan.edu.cn

^{*} Corresponding author: Hao-Chung Kuo, Department of Photonics and Graduate Institute of Electro-Optical Engineering, College of Electrical and Computer Engineering, National Yang Ming Chiao Tung University, Hsinchu, 30010, Taiwan, China; Semiconductor Research Center, Hon Hai Research Institute, Taipei, Taiwan, China, e-mail: hckuo@faculty.nctu.edu.tw

გ Open Access. © 2022 Xiaoyan Liu *et al.*, published by De Gruyter. 🕞 🕶 This work is licensed under the Creative Commons Attribution 4.0 International License.

solar battery [4,5], information encryption and decryption [6,7], visible light communication (VLC) [8,9], photonic memristor [10,11] as well as neural morphology calculation [12,13], as shown in Figure 1. Among them, the perovskite solar cell (PSC) has the advantages of high conversion efficiency, low cost, and simple preparation process, making it one of the most popular research fields in perovskite. In 2009, Kojima et al. applied the perovskite materials CH₃NH₃PbI₃ and CH₃NH₃PbBr₃ to quantum dot (QD)-sensitized solar cells for the first time, achieving a conversion efficiency of 3.8% [14]. With further research, the highpower conversion efficiency of more than 22% has been achieved [15,16]. In the field of VLC, perovskite materials are not only used as light emitters such as light-emitting diodes (LEDs) [17,18] and laser diodes [19] but also as light receivers such as PINs and photodetectors (PDs) [20,21]. Among them, perovskites combined with QDs have great research value due to their narrow emission and short fluorescence lifetime [9,22]. In addition, fluorescent materials such as carbon dots [23], inorganic QDs [24], and transition metal complexes [25] are used in information encryption and decryption, but they all have disadvantages such as poor luminescence performance and high cost. Fortunately, perovskite materials have the characteristics that the photoluminescence quantum yield (PLQY) of perovskite quantum dots (PQDs) exceeds 90%, and the full width at

half maximum of the PL peak is very narrow [26,27], making it a promising candidate for excellent fluorescent materials [28]. Sun et al. reported for the first time the use of PQDs to achieve information encoding, encryption, and decryption of full-color stimulus-response ink [7], which confirmed the application prospects of perovskite materials in information encryption. In recent years, the research of photonic memristor for photonic synapse and photonic neuromorphic calculation based on perovskite materials has been put on the agenda gradually. These studies will help simulate artificial synapses for data processing and promote the development of artificial intelligence. As an example, Pradhan et al. prepared photonic synapses based on graphene-PQDs (G-PQDs) superstructure materials, which successfully realized face recognition function through neural network calculation [29].

Based on optoelectronic properties, perovskite materials can be used in various optoelectronic devices. However, due to the complicated environment, the stability of the device will be reduced to a certain extent. Therefore, how to improve the stability of optoelectronic devices has become a hot topic. For humidity stability, moisture in the air is an important cause of accelerated device damage. Niu *et al.* added polyvinylpyrrolidone to methylammonium lead iodide (MAPbI₃) perovskite precursors and introduced hydrogen bonds to form high-performance PSCs [30].

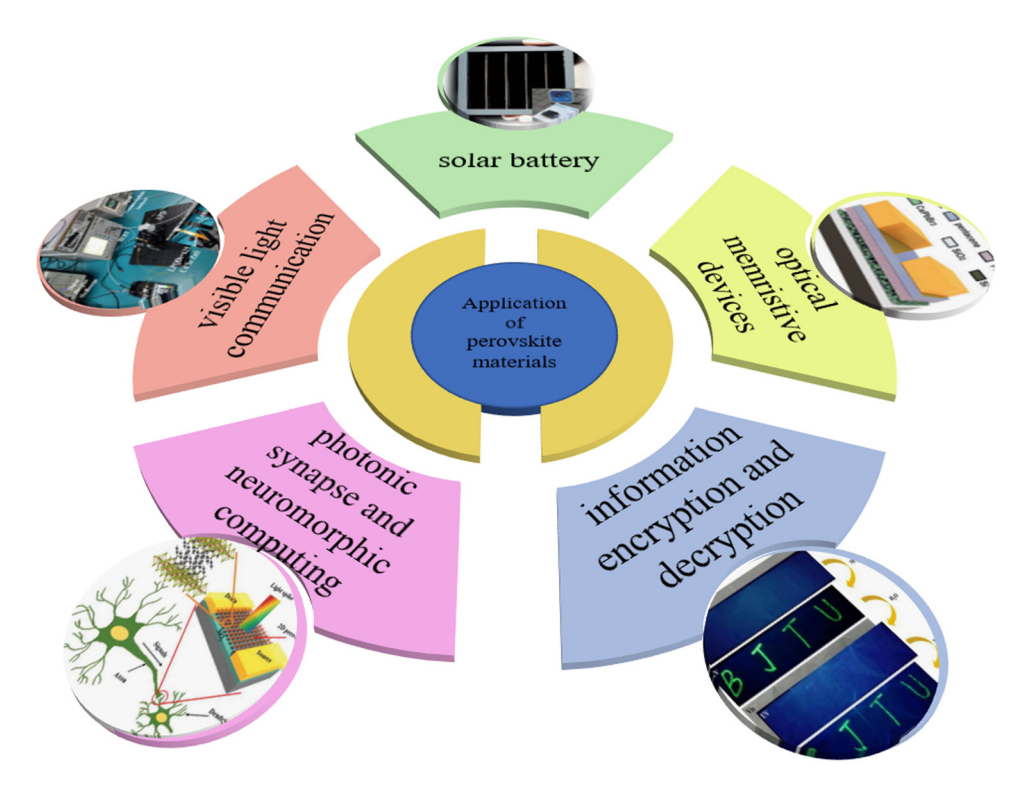


Figure 1: Schematic diagram of the application of perovskite materials in various fields.

The PSCs have a strong self-healing ability in an environment of high humidity (65 \pm 5% relative humidity), and the photoelectric conversion efficiency (PCE) of 20.32% is almost unchanged after working for 500 h. For the stability of ultraviolet (UV) light, the UV light will degrade perovskites and cause serious damage to PSCs. In this regard, Wang et al. used 2-hydroxy-4methoxybenzophenone to protect perovskite materials and used functional group interactions and intermolecular tautomerism to passivate molecular defects [31]. This approach can enhance the UV resistance of PSCs, resulting in long-term UV (UVa: 365 nm and UVb: 285 nm) stability. In addition, perovskite materials can also be physically or chemically encapsulated, for example, Hou et al. formed a composite of lead halide perovskite and metalorganic frameworks (MOFs) glass by liquid-phase sintering [32]. The glass is equivalent to the matrix, and the interfacial interaction can effectively stabilize the nonequilibrium perovskite phase. Therefore, the stability of the composite material in environments such as light, heat, and water can be improved. It is also a good way to stabilize perovskite precursors by utilizing the synergistic cooperation between functional groups. Li et al. used 3-hydrazinobenzoic acid (3-HBA) containing carboxyl (-COOH) and hydrazine (-NHNH) functional groups as stabilizers, which can effectively inhibit the oxidation of I[−], the amine-cation reaction and the desorption of organic cations [33]. The NiO_x-based inverted device can achieve an efficiency of 23.5% and still maintain 94% of the initial efficiency at the maximum power point after 601 h.

In recent years, there have been numerous reviews on the application of perovskite materials. For example, Liu et al. reviewed low-dimensional metal halide perovskites. With excellent photoelectric and mechanical properties, perovskites have potential applications in solar cells, lasers, and waveguides [34]. Choi et al. reviewed the applications of organic-inorganic hybrid halide perovskites in transistors, memory, and artificial synapses, especially highlighting the compositional flexibility of high-performance polymers, which are expected to become high-performance electronic-device materials in the era of massive data in the future [35]. Wang et al. summarized the applications of perovskites in non-volatile memory, especially resistive switches, and artificial synapses based on the flexible properties of perovskite materials [36]. Zhao et al. introduced the research progress of memristors based on the photoelectric properties of organic-inorganic halide perovskites, such as non-volatile storage, photo-related, and many other advanced applications [37]. Pecunia et al. summarized the current status, prospects, and explorations of lead-free metal halide perovskite photovoltaic (PV) cells,

and emphasized the potential room for progress in this direction, which is expected to achieve breakthroughs in high-performance PV cells [38]. Many reviews on perovskites have been reported from a variety of perspectives, such as perovskite synthesis, perovskite properties, various applications, and so on [34–38]. In addition to the application fields of the abovementioned perovskite materials, the excellent photoelectric properties of the perovskite materials also make them have application value in information encryption and decryption, VLC, and optical neuromorphic calculation of photon memristors. Therefore, on the basis of previous reviews, this work will further complement the research progress of perovskite in these latest cuttingedge areas to highlight huge development prospects in these emerging fields in recent years.

In this article, we mainly introduce the preparation methods, photoelectric properties, and applications of perovskite materials, especially information encryption and decryption, VLC with optoelectronic devices, and neuromorphic computing with photon memristive devices resulting from the advantages of perovskite materials. According to the different molecular structures of perovskites, the commonly used preparation methods of threedimension (3D) and low-dimension perovskites will be explained in turn. Based on the photoelectric characteristics of perovskites, we mainly elaborated their applications in solar cells, information encryption and decryption, VLC, and optical memristive devices. Perovskites have important research value in these latest cutting-edge fields and have excellent development prospects. Thus, we have compiled and listed the latest research progress in these areas in recent years, and briefly described and summarized the results. The application of perovskites in photon memristive devices is enabled to assist photonic neuromorphic calculations, showing its huge potential application prospects in the field of artificial intelligence in the future.

2 Preparation and properties of perovskite materials

2.1 Preparation methods

The synthesis of perovskite materials with excellent properties is an indispensable part of the preparation of corresponding devices. In this section, some preparation processes of perovskites that have emerged in recent years will be briefly overviewed according to the classification of 3D perovskites and low-dimension perovskites.

2.1.1 3D perovskites

In order to prepare 3D perovskites, there are two synthetic approaches that can be utilized, "bottom-up" and "top-down" [39-41]. The first approach is more commonly used, mainly by adjusting the composition at the molecular or atomic level, and synthesizing the final product through solution routes such as sol-gel chemical solution deposition and hydro/solvothermal synthesis. This approach has low costs and does not damage the sidewalls of the structure. However, because particles are distributed irregularly, it is difficult to obtain a regular size distribution. The top-down approach mainly uses focused ion beam milling or photolithography methods to carve away the bulk ferroelectric material and create coherently and continuously ordered nanostructures. The advantage of this process is that the size and shape of the synthesized nanostructures can be controlled precisely, and the drawback is the synthesis speed, and it is not suitable for volume patterned nanostructures [42]. The preparation methods of 3D perovskite and 3D hybrid perovskite are briefly investigated below.

A new tin-based 3D perovskite $\{en\}FASnI_3$ (en = ethylenediammonium, FA = formamidinium) (Figure 2a) was proposed and prepared by Ke *et al.* By introducing a cation, the stability of the tin-based perovskite in the

atmospheric environment can be significantly improved, as shown in Figure 2b, and the optoelectronic properties of the absorber prepared by the material are also optimized [43]. More recently, in order to obtain perovskite semiconductor devices that can work stably at above room temperature, an A-site cation [CH₃PH₃]⁺(methylphosphonium, MP) is employed to fabricate a lead-free 3D ABX₃ organicinorganic halide perovskite semiconductor MPSnBr₃. Attributed to the large volume and heavy mass of MP cation, MPSnBr₃ has a high Curie temperature [44]. At above room temperature, this material exhibits obvious ferromagnetic properties and the direct band gap of it is 2.62 eV. In addition, MPSnBr₃, as a multiaxial molecular ferroelectric, has 12 ferroelectric polar axes, much higher than other materials of the same type [45]. Due to this special feature, the polarization in each grain can be switched more easily between multiple directions to achieve an excellent ferroelectric performance [46]. Furthermore, Körbel et al. have screened the periodic table of the elements for hybrid organic-inorganic halide perovskites via highthroughput density-functional theory calculations [47]. By extracting the band gap energy and the effective masses, they have found that MPSnI₃ is one of the most promising compounds for PVs. It has a smaller band gap (1.18 eV) than MPSnBr₃, indicating more efficient light harvesting. In another study by Ozório et al., a density functional

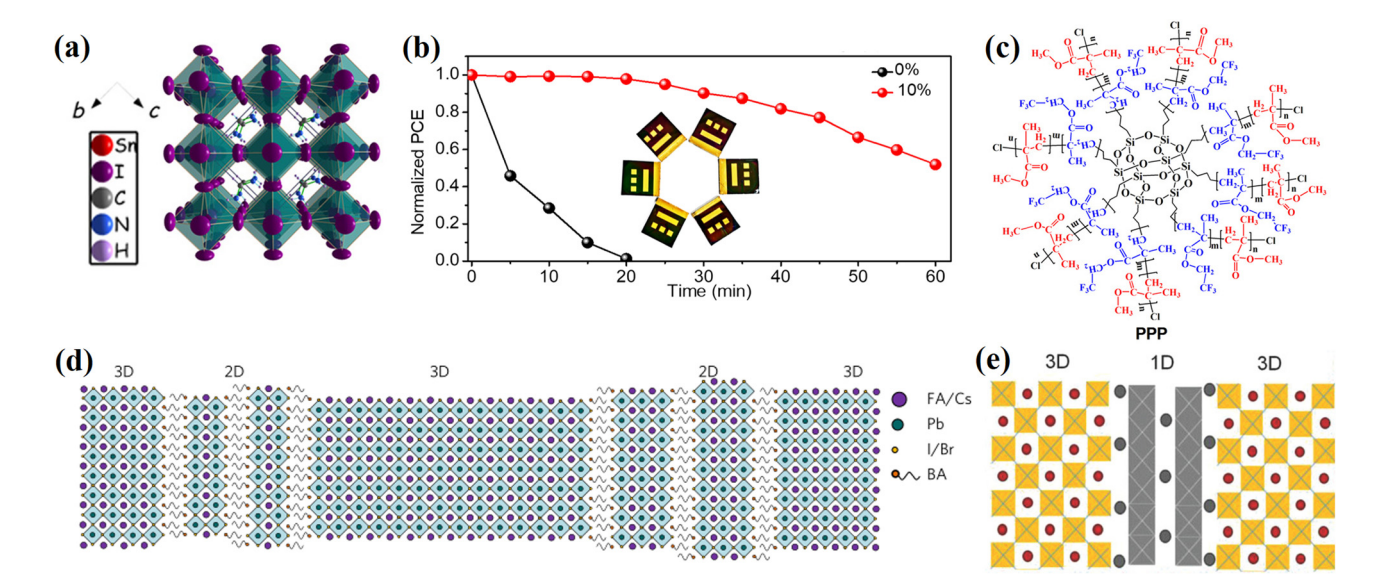


Figure 2: (a) Crystal structure of {en}FASnl₃. (b) Under constant conditions, an aging test of {en}FASnl₃-based unencapsulated solar cells with and without 10% en. Reproduced with permission from ref. [43]. Copyright 2017, American Association for the Advancement of Science. (c) Structural formula of PPP polymer for fabricating PPP-based 3D structure perovskite, reproduced with permission from ref. [50]. Copyright 2021, American Association for the Advancement of Science. (d) 2D–3D schematic diagram of heterostructured butylammonium-caesium-formamidinium lead halide perovskites, reproduced with permission from ref. [51]. Copyright 2017, Springer Nature. (e) Schematic diagram of the heterostructural 1D–3D hybrid perovskite film by introducing PZPY into lead halide 3D perovskites, reproduced with permission from ref. [52]. Copyright 2018, Wiley-VCH.

theory investigation of the MPSnI₃ perovskite phases was reported [48]. By calculating the enthalpy of formation, they found that MPSnI₃ has a higher thermodynamic stability at 0 K compared with the FASnI₃ phase. However, due to the weaker structural cohesion, the MPSnI₃ structures can be more affected by moisture and oxygen-rich environment. Currently, the research on MPSnI₃ is only in the theoretical calculation, and its preparation and experiment still need to be further studied. Without organic ligand and toxicity elements, a facile antisolvent method at room temperature is introduced by Wu et al. to synthesize novel lead-free CsAgCl₂ perovskite microcrystals, which exhibit excellent air, thermal, and light stability [49]. Cao et al. designed a 3D star-shaped polymer (polyhedral oligomeric silsesquioxane-poly(trifluoroethyl methacrylate)-bpoly(methyl methacrylate) (PPP)) as a novel modulator to regulate perovskite film crystallization, as shown in Figure 2c [50]. The core of the star-shaped PPP can offer the PPP-based perovskite 3D structure stability. Some researchers found that cation engineering in 3D perovskite absorbers can lead to reduced degradation. As a consequence, two-dimension (2D) Ruddlesden-Popper phase layered perovskites are explored to improve device stability. Take $(RNH_3)_2(A)_{n-1}BX_{3n+1}$ as an example, RNH_3 are large alkylammonium cations. Wang et al. prepared a kind of 2D-3D heterostructured perovskites by introducing *n*-butylammonium cations into FA_{0.83}Cs_{0.17}Pb(I_vBr_{1-v})₃ 3D perovskites, as shown in Figure 2d. The use of this material can improve the performance and stability of PSCs [51]. Inspired by the 2D-layered perovskites where the A site molecule is substituted by large alkyl ammonium cations, Fan et al. innovatively introduced a controlled amount of one-dimension (1D) 2-(1H-pyrazol-1-yl)pyridine (PZPY) into the 3D perovskite precursor system to synthesize heterostructural 1D-3D perovskite for preparing 1D-3D perovskite solar cells, as shown in Figure 2e, which possess thermodynamic self-healing ability, high efficiency, and long-term stability [52].

2.1.2 Low-dimension perovskites

Compared with 3D perovskites, low-dimension perovskites exhibit unique electrical and optical characteristics such as quantum confinements, anisotropic geometry and large surface to volume ratio, which make them promising candidates for next generation electronic and optoelectronic applications. Therefore, most efforts are made to investigate the synthesis of low-dimensional perovskites with high-quality, including 2D nanoplatelets (NPLs), 1D nanowires (NWs), and zero-dimension (OD) QDs.

For 2D materials, the mechanical exfoliation method is an easy-to-operate preparation method, but it can only be used for the preparation of layered perovskites, there is no way to control the morphology of the product, and the yield is low. In order to overcome these shortcomings, solution-phase growth and chemical vapor deposition (CVD) are more used in the preparation of 2D perovskites [5]. In 2014, Ha et al. presented for the first time a synthesis method for perovskite family NPLs with thickness from several atomic layers to several hundred nanometers, which has sizes from 5 to 30 µm and an electron diffusion length exceeding 200 nm. The corresponding schematic of the synthesis setup using a home-built vapor-transport system is shown in Figure 3a [53]. To crystallize MAPbI₃ rapidly at room temperature without the participation of strongly coordinating aprotic solvents, a solvent system with a low-boiling point and low viscosity was introduced by Noel et al. By using this kind of solvent, pinhole-free films with uniform coverage and compactness can be manufactured, which exhibits good photoelectric properties [54]. Another method of anti-solvent-extraction technology can also be employed to prepare uniform pinhole-free CsPbI₂Br film, which possesses good stability, even in a high-temperature pressure environment and continuous light infiltration under the conditions of maximum power point tracking. Figure 3b shows the solvent engineering procedure for preparing the uniform and dense perovskite film [55]. With the need for the actual application, the large-scale synthesis of highquality perovskite NPLs is desired. Tong et al. proposed a versatile, polar-solvent-free, single-step approach without a polar solution, which can synthesize $CsPbX_3$ (X = Br or I) NPLs on a large scale, and the NPL thickness can be tuned by direct ultrasonication to the related precursors [56].

With the continuous deepening of perovskite research, researchers are pursuing high purity and high-stable 2D perovskite [57–59]. Duan et al. proposed a multistep solution-processing strategy to synthesize CsPbBr₃ perovskite films with high purity. The phase conversion of perovskite can be achieved by adjusting the number of deposition cycles of a CsBr, which is conducive to the formation of monolayer and vertical-aligned grains. During the synthesis process, a clear crystal structure transformation can be observed, shown in Figure 3c [57]. Studies have shown that retarding the crystallization rate of perovskite can improve the stability and efficiency of the perovskite-based device [58-61]. A method of hydrogen bonding formed by adding poly(vinyl alcohol) (PVA) to the FASnI₃ perovskite precursor solution was introduced to retard the crystalline rate of perovskite by controlling the growth of FASnI₃ perovskite, thereby reducing the trap density of the resulting

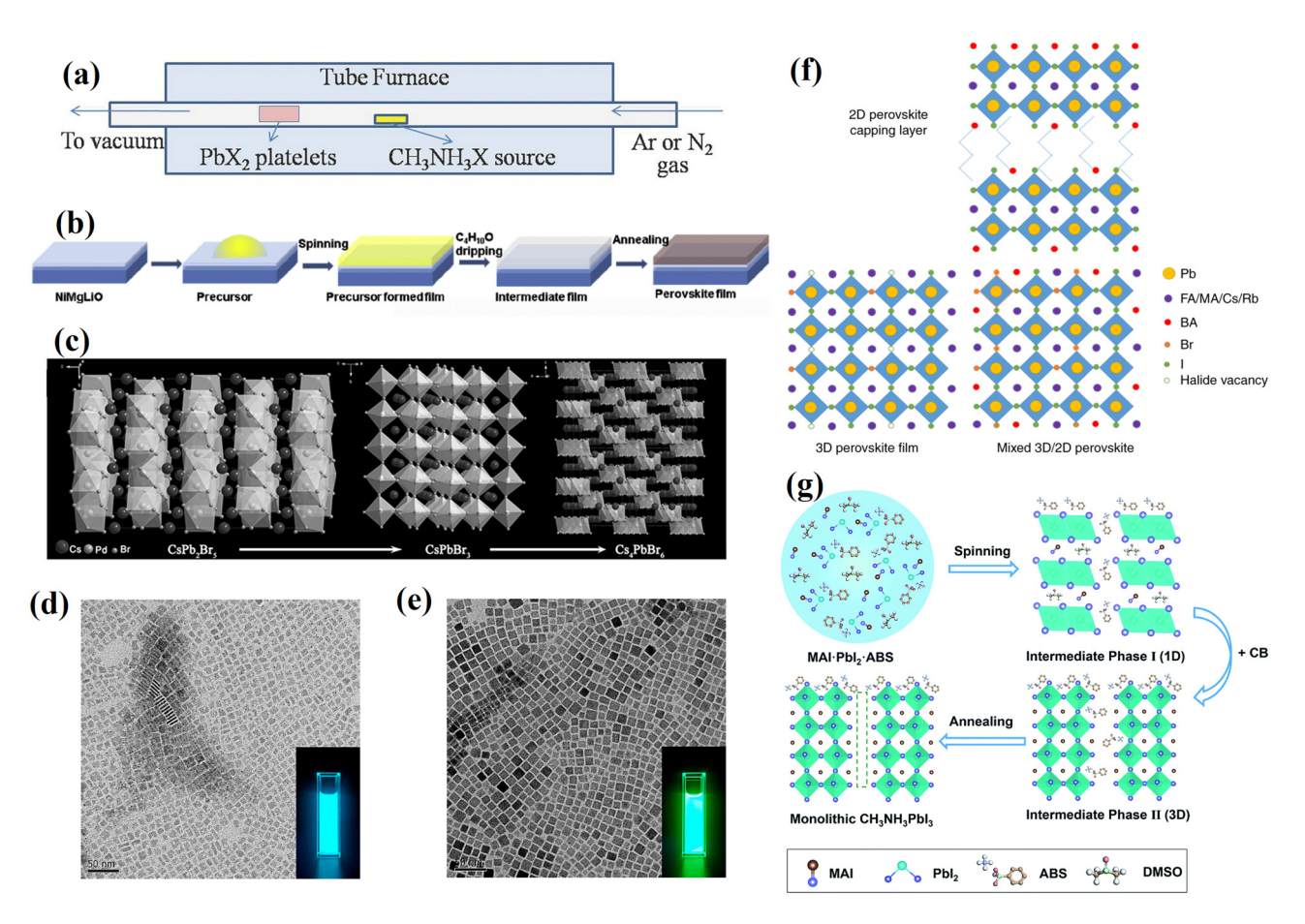


Figure 3: (a) The schematic of the synthesis setup for 2D perovskite nanoplate using a home-built vapor-transport system, reproduced with permission from ref. [53]. Copyright 2014, Wiley-VCH. (b) The solvent engineering procedure for preparing the uniform and dense inorganic CsPbl₂Br perovskite film, reproduced with permission from ref. [55]. Copyright 2018, Elsevier. (c) A clear crystal structure transformation in the synthesis process of the all-inorganic cesium lead bromide halide, reproduced with permission from ref. [57]. Copyright 2018, Wiley-VCH. TEM images of CsPbBr₃ PNCs synthesized at (d) 120°C (NPLs) and (e) 185°C (nanocubes), reproduced with permission from ref. [60]. Copyright 2021, American Chemical Society. (f) Schematic of 2D/3D perovskite film formed *via* the dimensionally graded perovskite formation method, reproduced with permission from ref. [61]. Copyright 2021, Springer Nature. (g) Schematic reaction process of monolithic CH₃NH₃Pbl₃ grain from the precursor to monolithic perovskite grains, reproduced with permission from ref. [62]. Copyright 2019, The Royal Society of Chemistry.

FASnI₃-PVA perovskite film and improving its compactness. Meanwhile, it exhibited striking long-term device stability [59]. Another method of a one-pot hot injection is employed by controlling the reaction temperature to synthesize CsPbBr₃ NPLs, then neighboring NPLs make facet-to-facet contact and then fuse into larger 2D NPLs (2–5 times) without defects, which is used to fabricate photoconversion device with long-term performance stability. Figure 3d and e shows two different dimensional CsPbBr₃ perovskite nanocrystals (PNCs) synthesized at different temperatures [60]. In 2021, Yang *et al.* proposed a multifunctional 2D perovskite passivation approach named the dimensionally graded perovskite formation approach to prepare low-photovoltage-loss PSCs and enhance the stability of the solar-cell device. The schematic of 2D/3D

perovskite film formed *via* this approach is shown in Figure 3f [61]. To further grow large-grain and less-defect perovskite films, Yang *et al.* introduced ammonium benzenesulfonate (ABS) into MAPbI₃ precursor, as shown in Figure 3g. During the entire reaction process, the presence of the ABS can slow down the crystallization process and improve the film quality. In addition, positive and negative charged defects are also effectively passivated for the zwitterion-structured ABS which remains in the perovskite [62]. Chu *et al.* combined large cation ethylammonium with PEA₂(CsPbBr₃)₂PbBr₄ (PEA = phenylethylammonium) perovskite. Through decreasing the Pb-Br orbit coupling and increasing the band gap for blue emission, efficient and spectra stable blue perovskite LEDs were fabricated successfully [63].

The synthesis method of 1D perovskite can be divided into solution-phase synthesis, vapor-phase synthesis as well as combined solution-phase and vapor-phase synthesis methods. For example, Yang et al. reported a simple and easily scaled synthesis method at room temperature without any organic solvent and expensive alkyl halide to prepare 1D organic-inorganic hybrid perovskite microbelt (AD) Pb_2Cl_5 (AD = acridine), and the process is shown in Figure 4a. The obtained low-dimension perovskite has high water stability and luminescent properties, and exhibits optical properties such as up-conversion fluorescence, polarized photoemission, and optical waveguide performances with a low loss coefficient during propagation. It has great potential to be applied in optical communication micro-devices [64]. Lately, Hu et al. synthesized a new 1D chiral hybrid perovskite material through a solution

process, which was determined to be a previously unknown low-dimensional hybrid perovskite (R)-(-)-1cyclohexylethylammonium/(S)-(+)-1 cyclohexylethylammonium) PbI₃ shown in Figure 4b [65]. The exploration of this type of material will help to understand some phenomena such as photo-galvanic effects, electric field, and chiral enantiomer-dependent Rashba-Dresselhaus splitting. In addition, water-stable 1D hybrid lead-free tin and lead halide perovskites were synthesized by a solution process. The SnCl₂·2H₂O and 1,8-diamino octane (2:0.5) were added to a mixed solution of hydrogen iodide and hypophosphorous acid (H₂PO₂) in a volume ratio of 5:8 to prepare (DAO)Sn₂I₆ (DAO, 1,8-octyldiammonium), which is water stable for more than 15 h [66]. Latest, a one-pot solution process anisotropic growth was introduced to synthesize super long monocrystalline CsPbBr₃ perovskite wires, which

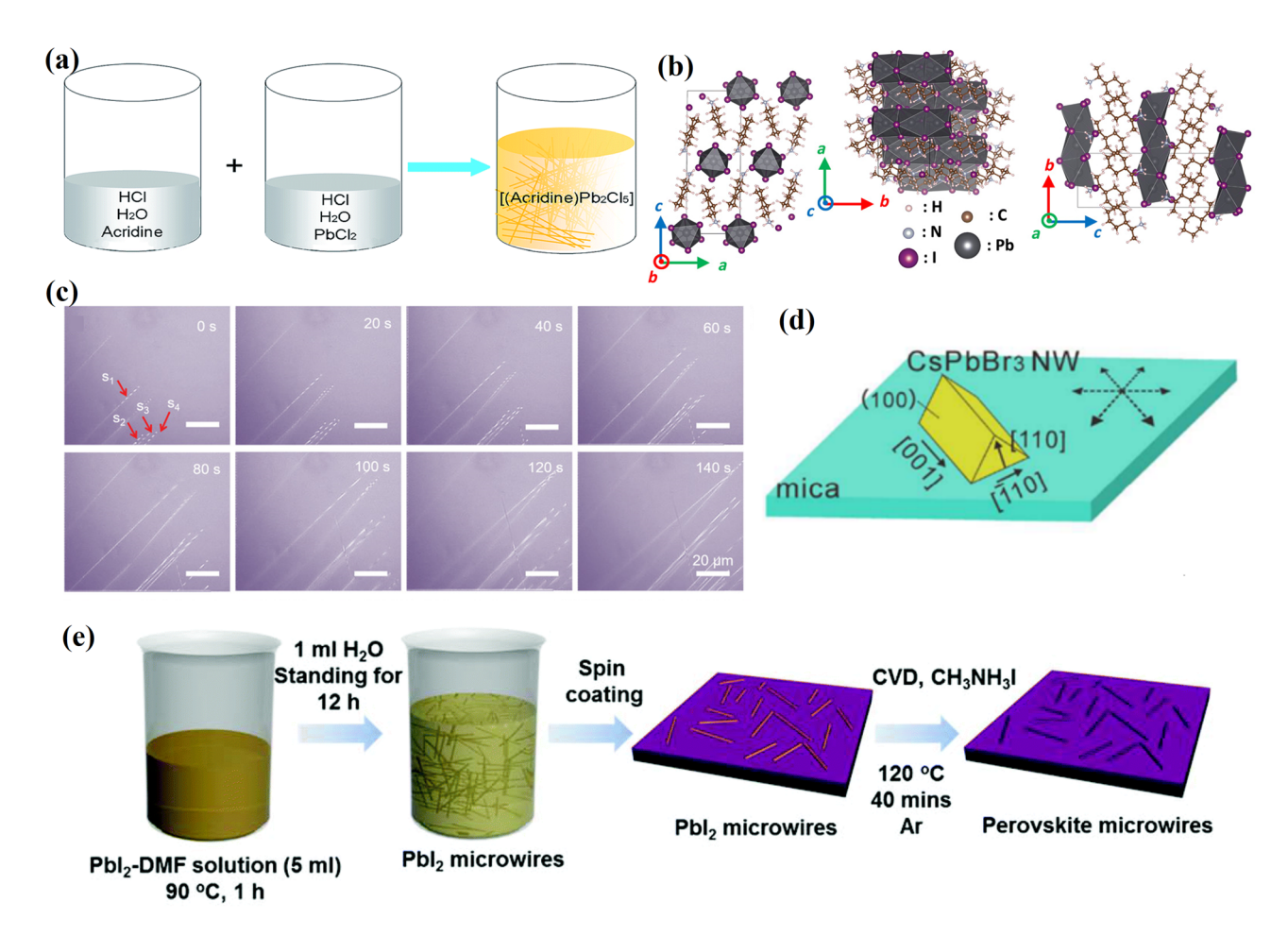


Figure 4: (a) The facile synthesis process of organic–inorganic hybrid perovskite-AD crystals in aqueous solution at room temperature, reproduced with permission from ref. [64]. Copyright 2019, The Royal Society of Chemistry. (b) A diagram of the structure of the 1D perovskite, reproduced with permission from ref. [65]. Copyright 2020, American Association for the Advancement of Science. (c) Optical microscope photograph for *in situ* monitoring wire growth, reproduced with permission from ref. [67]. Copyright 2021, Wiley-VCH. (d) A schematic illustration of the epitaxial growth of CsPbBr₃ NWs on mica, reproduced with permission from ref. [68]. Copyright 2017, American Chemical Society. (e) Schematic of the solution process to fabricate PbI₂ microwires and the vapor phase conversion process to transfer PbI₂ into hybrid perovskite NWs, reproduced with permission from ref. [70]. Copyright 2016, The Royal Society of Chemistry.

exhibit well-defined morphology and a high aspect ratio over 10⁵ [67]. The optical microscope photograph for in situ monitoring wire growth is shown in Figure 4c. In contrast, 1D perovskites prepared from the vapor-phase synthesis method have less defect density and higher crystallinity. In 2017, Chen et al. first reported the direct epitaxial growth of CsPbBr3 NWs and microwires with controlled crystallographic orientations on both p-mica and m-mica, which was carried out in a home-built CVD reactor, the related A schematic illustration is shown in Figure 4d [68]. The wires typically have a width of ~1 µm and a length of tens of micrometers. Very recently, a noncatalytic CVD growth method was introduced by Hossain et al. to prepare all-inorganic CsPbX₃ perovskite NWs [69]. Besides, mixed preparation methods, such as solution-vapor growth, solution-vapor-solid growth were studied to make high-quality perovskite NWs, which enabled the growth of anisotropic perovskites [70]. Figure 4e shows a schematic of the process to synthesize hybrid perovskite NWs.

The solid-state reaction method is a traditional method for synthesizing perovskite nanopowders, but in order to obtain homogenized colloidal nanocrystals (NCs), the liquid-phase synthesis method is widely used. Among them, the hot injection (HI) method and the ligandassisted reprecipitation (LARP) method are the two most developed OD perovskite fabrication methods [71]. In 2015, Protesescu et al. proposed a HI method that can synthesize the solution-processed monodisperse CsPb X_3 (X = Cl, Br, I, mixed Cl/Br, or Br/I systems) NC [72]. NCs are also known as nanocrystal QDs. This research shifts the focus from hybrid organic-inorganic lead halides MAPbX₃ to the previously unresearched all-inorganic cesium lead halide perovskites (CsPbX₃) colloidal nanomaterials. However, the unpurified ODs obtained by this method will be transformed into the orthorhombic phase within a few days. In 2016, Swarnkar et al. improved the preparation method reported by Protesescu et al. and stabilized the CsPbI₃ QDs in the cubic phase in an ambient environment by purifying the QDs [73]. The prepared a-CsPbI₃ QDs are phase-stable for months in ambient air and even at cryogenic temperatures. Lately, Yang et al. presented a modified HI method of one-step synthesis strategy for CH₃NH₃PbBr₃ PQDs. The colloidal solution obtained by this method has bright green emission, and the particle size of the PQDs is less

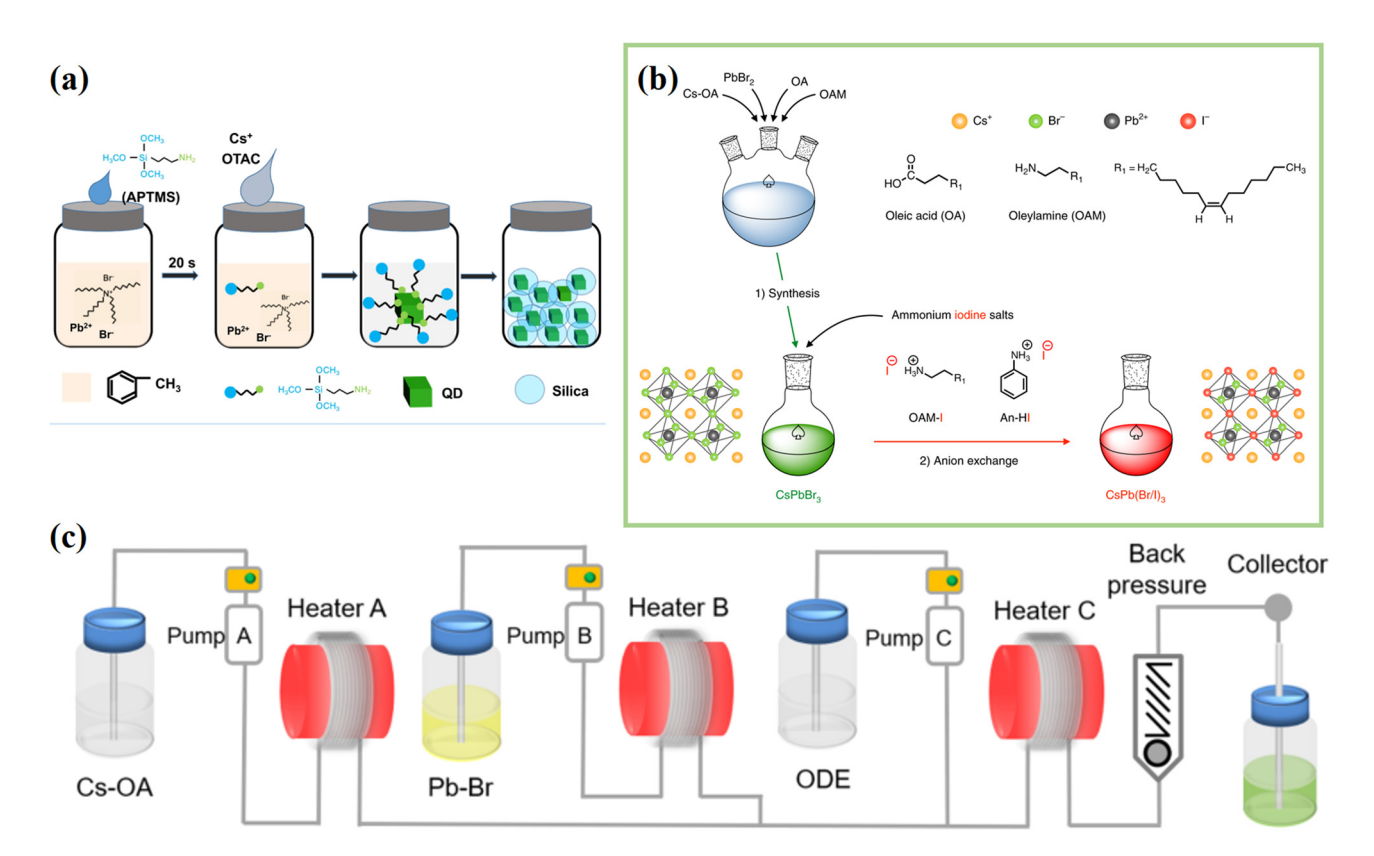


Figure 5: (a) Preparation diagram of CsPbBr₃ PQDs solid powder, reproduced with permission from ref. [76]. Copyright 2021, Elsevier. (b) Schematic diagram of anion exchange based on long alkyl ammonium and aryl ammonium, reproduced with permission from ref. [79]. Copyright 2018, Springer Nature. (c) Schematic diagram of the microfluidic system for producing CsPbBr₃/Cs₄PbBr₆ PNCs, reproduced with permission from ref. [81]. Copyright 2021, Elsevier.

than 10 nm [74]. These strategies can improve the stability or optical properties of PQDs to a certain extent. Yet, the synthesis of PQDs by HI requires a high temperature, inert environment, and some other conditions [75].

LARP is another popular synthesis method because it can be carried out in an atmospheric environment through an ordinary mixing process without heating equipment or inert gas protection. Guo and co-authors employed 3aminopropyltrimethoxysilane as ligands to prepare largescale stable CsPbX₃ PQDs at room temperature [76]. Figure 5a is the preparation diagram of CsPbBr₃ PQDs solid powder. In order to further overcome the poor stability of OD perovskites, Guo and co-authors proposed thioacetamideligand-mediated synthesis to prepare novel CsPbBr₃-CsPbBr₃ homostructured NCs through a facile room-temperature reprecipitation method [77]. Because of consuming a large amount of toluene and N, N-dimethylformide, LAPP might lead to low stability, a mixture of morphologies [78]. For the sake of improving the quality and properties of OD perovskite, many other methods were explored for the synthesis of high-quality and high-performance perovskite with few defects. For instance, an atomic exchange method was introduced by Chiba et al. to prepare red PQDs, which converted the original green CsPbBr3 QDs into red QDs through the halide-anion-containing alkyl ammonium and aryl ammonium salts, as shown in Figure 5b [79]. The material exhibits a strong red shift and higher PLQY from green emission to a deep-red emission at 649 nm. Another approach of comprehensive defect suppression in perovskite NCs, that is, an ideal one-dopant alloying strategy was designed by Kim et al., which can produce monodisperse colloidal perovskite NCs with smaller sizes

and fewer surface defects [80]. As is well-known, the synthesis of large-scale complex NCs is difficult. In 2021, a microfluidic system, as shown in Figure 5c, was applied by Bao *et al.* for a simple, continuous, and stable synthesis of large-scale CsPbBr₃/Cs₄PbBr₆ complex NCs with a high PLQY of up to 86.9% [81].

2.2 Optical and electrical properties of perovskites

2.2.1 Optical properties of perovskites

Perovskite is a direct band gap semiconductor, which exhibits strong absorption of up to 10⁵ cm⁻¹ from UV to visible light. Thus, an extremely thin perovskite film can achieve complete light absorption, which is beneficial to carrier collection and further design of device structure. In addition, the perovskite band gap is within 1.4–3.0 eV, and the light absorption and emission can just cover the entire visible light region, that is why perovskite has broad application prospects. Figure 6 shows the corresponding spectra of different perovskite materials in the visible range [72], in which the spectral range of organic perovskite MAPbX₃ is 390–790 nm, and the spectral range of inorganic perovskite CsPbX₃ is about 400–710 nm. According to the corresponding calculation, the band gap of the perovskite is in the range of 1.4–3.0 eV.

As the composition changes, the perovskite absorption and fluorescence spectra can be continuously adjusted. For instance, Protesescu *et al.* developed a series of CsPbX₃

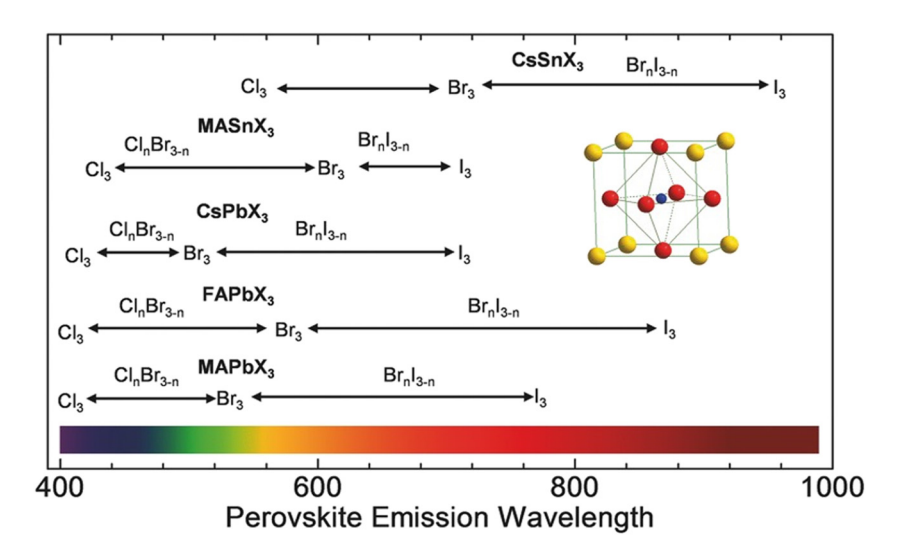


Figure 6: Spectral absorption and emission ranges of different perovskite materials in the visible light region, reproduced with permission from ref. [82]. Copyright 2017, Wiley-VCH.

(X = Cl, Br, I) perovskite nanoparticles (NPs) with different components and realized the continuously adjustable fluorescence spectrum from 410 to 710 nm in the visible light range (Figure 7) [72]. Figure 7a shows the tunable luminescence color of the perovskite solutions under the excitation light of 365 nm. Figure 7b and c shows the adjustable optical absorption and emission spectra of CsPbX3 in the entire visible spectrum by adjusting their composition and particle size. According to Figure 7b, it can be observed that the half-width of the perovskite PL peak is very narrow, between 12 and 42 nm, which fully proves that the material has high monochromaticity. The optical performance adjustment between the same type of perovskite can be achieved through ion exchange, and this can also be achieved between different types of perovskites. Wang et al. prepared $FA_{0.33}Cs_{0.67}PbBr_{3-x}I_x$ (0 $\leq x \leq$ 3) organic-inorganic hybrid perovskite through the solution method and adjusted its PL performance by changing the proportion of halogen ions [83].

Compared with 3D materials, low-dimensional semiconductors such as ODs and 2D NWs have different optical properties. Under the quantum confinement effect, QDperovskites and 2D nano-perovskites have variable PL peak positions and absorption edges and have better light stability than 3D-structured perovskites. In addition, PQDs have the advantage of defect tolerance. Although the system has a large number of inherent structural defects, its optical properties still have unique advantages. In recent years, there have been many research reports on PQDs. Including all-inorganic materials and organic-inorganic hybrid materials, almost all types of PQDs have been reported. Furthermore, some experts have discovered that

a well-designed hybrid 2D/3D perovskite is a combination of ideal optoelectronic properties and moisture resistance stability, which can cover the advantages of 2D and 3D perovskites.

For perovskite nanomaterials, because of the existence of quantum effects, the optical properties of the perovskite nanomaterials will change to a certain extent with the thickness of the perovskite nanomaterials. Taking MAPbI₃ as an example, Liu et al. synthesized MAPbI₃ nanosheet structures with different thicknesses by solution method and tested PL of samples with different thicknesses [84]. The results show that as the nanosheets increase from a single layer to 10 layers, the PL peak position has a significant redshift from 724 to 755 nm. From a single layer to a bulk phase, the band gap shift can reach 100 meV, which indicates that the thickness of the perovskite nanosheet has a great relationship with its optical properties.

2.2.2 Electrical properties of perovskites

Perovskite has strong carrier transport capacity and higher carrier mobility comparable to GaAs and Si inorganic materials. The carrier mobility of polycrystalline thin-film perovskite is 1–30 cm² V⁻¹ s⁻¹. Because of high purity, few grain boundaries, and low defect density, mobility can reach more than 200 cm² V⁻¹ s⁻¹ in the perovskite singlecrystal material [85].

Yang et al. observed that the ion conductivity in MAPbI₃ was significantly higher than the electronic conductivity, indicating the importance of ion transport in

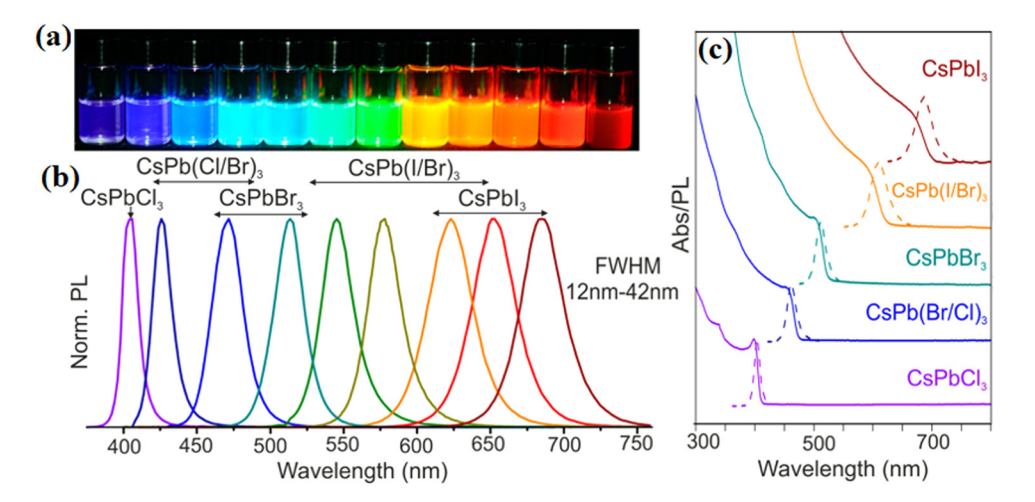


Figure 7: (a) The luminescence color of the perovskite solution under UV light ($\lambda = 365 \text{ nm}$). (b) The PL fluorescence peak position change of the corresponding component (except for the CsPbCl₃ excitation wavelength of 350 nm, the rest are all 400 nm). (c) The absorption spectrum of the corresponding component. Reproduced with permission from ref. [72]. Copyright 2015, American Chemical Society.

perovskite [86]. They tested the electrical data obtained by pure phase doping with a small amount of MAPbI₃. Based on a variety of characterization methods, Senocrate et al. finally determined that the conductive ion in MAPbI₃ is I⁻, that is, the ion conductance in perovskite is mainly contributed by halogen ions [87]. Due to the increase in I⁻ vacancies caused by Na⁺ doping, both the ion conductivity and the electronic conductivity increased by more than one order of magnitude after doping, so it can be inferred that I plays an important role in ion conductivity. In addition, the conductivity of perovskite is not only related to temperature and I₂ partial pressure but also related to light. Kim et al. found that under light conditions, compared with the dark state, the electronic conductance and ion conductance of perovskite increased significantly, and the ion conductance increased by three orders of magnitude [88]. That is because light effectively increases the chemical potential of I-, making it more prone to migration. As the light intensity increases, ion conductance and electronic conductance will continue to increase.

3 Latest cutting-edge applications of perovskites

Perovskite materials have many excellent optoelectronic properties such as high electron mobility, suitable band gap, strong light absorption, and high luminous efficiency. Moreover, perovskite nanomaterials such as NWs and nanosheets usually have very high crystalline quality, small size, and superior performances. These characteristics make it have broad application prospects in many fields such as solar cells, information decryption and encryption, VLC, and memristors for memory and computing as well as artificial synaptics. The following mainly introduces the applications of perovskite materials in the abovementioned aspects in detail.

3.1 Solar battery

A solar cell is a device made of a certain light-absorbing material that can directly absorb sunlight and convert light energy into electrical energy. In physics, it is referred to as PV. In general, solar cells have experienced a second revolution in the historical sense: the first generation is based on silicon wafers (monocrystalline silicon and polycrystalline silicon), of which the power conversion efficiency

is 15–20%, but these batteries are more expensive because of their high cost of processing and raw materials; the second generation is based on amorphous silicon, copper indium gallium selenide (CIGS), and cadmium telluride (CdTe), but there are still problems with low conversion efficiency and module stability. PSCs are expected to become mainstream for third-generation solar cells in the next few years because of their low processing cost, easy manufacturing, and large-area production using electrospray technology [89].

Hybrid halide perovskites are commonly used materials in solar cells. A in the ABX₃-structure hybrid halide perovskite is usually a stable organic cation, such as HC (NH₂)₂ (FA) and CH₃NH₃ (MA). At present, formamidine lead iodide (FAPbI₃) has attracted the attention of scholars due to its excellent properties and broad application prospects. Based on density functional theory, Pachori et al. conducted experiments using PBE-sol and WC-GGA exchange-correlation potentials [90]. The structural, electronic, optical, and thermal properties of FAPbI₃ were successfully verified. FAPbI3 is a direct band gap semiconductor (1.30 eV) with an absorption coefficient much higher than $10^4 \, \text{cm}^{-1}$ in the visible region. At the same time, it shows higher compressibility and low-temperature dependence, which can improve the stability of PV devices. In addition, they also studied the physical properties of the tin-based formamidinium (FASn X_3 , X = I, Br, Cl) for the first time [91]. It was found that all these compounds have similar band gaps, high thermal and elastic stability, and high dielectric constants and absorption coefficients. This research is conducive to the search for more stable and more efficient hybrid compounds composed of lead-free perovskites, thereby realizing higher performance solar cells.

For the simulated efficiency, MonikaPachori et al. used the full potential linearized augmented plane wave method to study the structure and properties of FAPbI₃ and fabricated FAPbI₃ PV devices [92]. According to the energy band structure, FAPbI3 has a direct band gap of 1.44 eV at the symmetry point R(0.5, 0.5, 0.5). The stability of the structure mainly depends on the strong hybridization of the s orbital of Pb atom and the p orbital of I atom in the valence band. It was found that when the materials in the buffer layer were ZnS and CdS, the FAPbI₃ thin-film solar cells had the highest efficiencies, which were 20.48 and 20.77%, respectively. Since the Pb element will cause certain damage to the environment, MonikaPachori et al. used Analysis of Microelectronic and Photonic Structuresone dimensional (AMPS-1D) to analyze the FASnI₃ PV device [93]. Experiments show that FASnI₃ has semiconductor properties. When the temperature of the FASnI₃ absorption layer is 300 K and the thickness is 300 nm, the spectral limit maximum efficiency is 28.37%.

Moreover, MAPbI₃ has excellent PV properties, becoming one of the main research areas in solar cells. MAPbI₃ has the characteristics of high dielectric constant and cubic structuretetragonal phase transition. So it is speculated that it has ferroelectric properties. In this regard, Kim et al. used piezoelectric force microscopy (PFM) to study the ferroelectric polarization behavior of MAPbI₃ [94]. They sequentially employed positive and negative polarization processes and measured the PFM phase in both darkness and illumination. The study found that MAPbI₃ has spontaneous polarization behavior. confirming its ferroelectric properties. Positive polarization can further promote electrical polarization, while negative polarization weakens electrical polarization. Under strongly polarized electric fields, light-induced polarization is prominent. Positively polarized light-induced polarization can provide efficient electron channels, which are beneficial for charge transport and collection. Jia et al. incorporated the ferroelectric polymer P(VDF-TrFE) into the absorber layer of solar cells [95]. The ferroelectricity of P(VDF-TrFE):MAPbI₃ hybrid films was observed by PFM. Applying a bias voltage across the ferroelectric thin films can tune the PV properties of PSCs. The results showed that the PCE of MAPbI₃-based PSCs increased from 13.4 to 17.3%. Taya et al. used Sn and Ge to partially or completely replace Pb, which can greatly improve the absorption of solar cells [96]. By adjusting the Sn and Ge doping concentrations in MAPb_{1-x-v}Sn_xGe_vI₃ [(x, y) = (0, 0.5), (0.25, 0.25), (0.5, 0)], the band gap can be reduced from 1.16 to 0.77 eV, while improving the light absorption coefficient in the visible region and even the mid-infrared region.

Besides hybrid organic–inorganic halide solar cells, inorganic perovskite-PSCs are also a hot research direction. Next we will briefly introduce the latest achievements of several solar cells based on inorganic perovskite materials, and list their photoelectric parameters in Table 1.

Table 1: PV parameters of the inorganic perovskite-based solar cells

Inorganic perovskite	PCE (%)	J _{SC} (mA cm ⁻²)	V _{oc} (V)	Ref.
$CsPb(Br_xI_{1-x})_3$	6.5	10.9	_	[97]
CsPbBrl ₂	12.2	14.22	1.20	[98]
CsPbI ₂ Br	16.70	15.64	1.30	[99]
CsPbl ₂ Br	16.93	14.71	1.38	[100]
CsPbI ₃	18.02	20.30	1.125	[102]
CsPbI _{2.1} Br _{0.9}	18.06	12.77	1.89	[101]
$CsPb(Br_xI_{1-x})_3$	18.14	1.22	18.16	[104]
CsPbI ₃	20.08	20.76	1.148	[103]

According to reports, the PCE of organic-inorganic hybrid PSCs has surpassed 23% [57], and the PCE of allinorganic PSCs has also exceeded 17%. Compared to organicinorganic hybrid PSCs, inorganic perovskite materials have become one of the hot spots in the research field of PSCs due to their good thermal stability. Beal et al. applied the prepared CsPb(Br_xI_{1-x})₃ inorganic lead halide perovskite material to a solar cell, which has a layered structure [97]. It can be obtained through spectral analysis that the inorganic lead halide perovskite material can make the light absorption layer of the battery have better light absorption performance and thermal stability. The disadvantage is that the PCE of solar cells based on inorganic lead halide perovskite CsPb $(Br_xI_{1-x})_3$ is only 6.5%. There is still a certain gap with the efficiency of organic-inorganic hybrid perovskite. In order to obtain practical applications, all-inorganic PSCs must be continuously optimized.

Inorganic CsPb X_3 (X = Cl, Br, I) PNCs not only have the same good optoelectronic properties as bulk materials but also have the properties of nanomaterials. For example, the colloidal ink has an adjustable gap and easy handling characteristics, which makes it easy for integration into many kinds of electronic devices and compatible with printing technology. Liu et al. used a simple hexane/ ethyl acetate (MeOAc) solvent treatment method to change the number of ligands around CsPbBrI₂ NCs [98]. Figure 8a also demonstrated the effect of the number of ligands on the film, which further affects the performance of the solar cell. Then, the nuclear magnetic resonance (NMR) internal standard method was used to accurately quantify the number of ligands. The final measured reverse scan current density-voltage (J-V) curve is shown in Figure 8b. By controlling the amount of ligand, the trapped state density was reduced by about 4 times, the carrier mobility was increased by nearly 15 times, and the PCE of 12.2% was finally realized. This is almost the highest reported performance of the hybrid halide CsPbX₃ PNCs solar cell.

Very recently, remarkable achievements have been made for solar cells based on perovskites. He *et al.* mixed passivation of organic phenethylammonium bromide and inorganic cesium bromide for the first time, and specifically studied its effect on all-inorganic perovskite (CsPbI₂Br) solar cells [99]. The structure diagram of the experimental device is shown in Figure 8c, which is consisted of Glass/ITO/ZnO/SnO₂/CsPbI₂Br/(PEABr + CsBr)/Spiro-OMeTAD/Ag. Different passivation mechanism treatments can obtain different efficiencies. After experimental verification, the characteristics of the best device with an optimized PEABr + CsBr are measured, which have a circuit current density (I_{sc}) of 15.64 mA cm⁻², an open-circuit voltage (V_{oc}) of 1.30 V, an excellent fill factor (FF) of 0.82, and a high PCE of

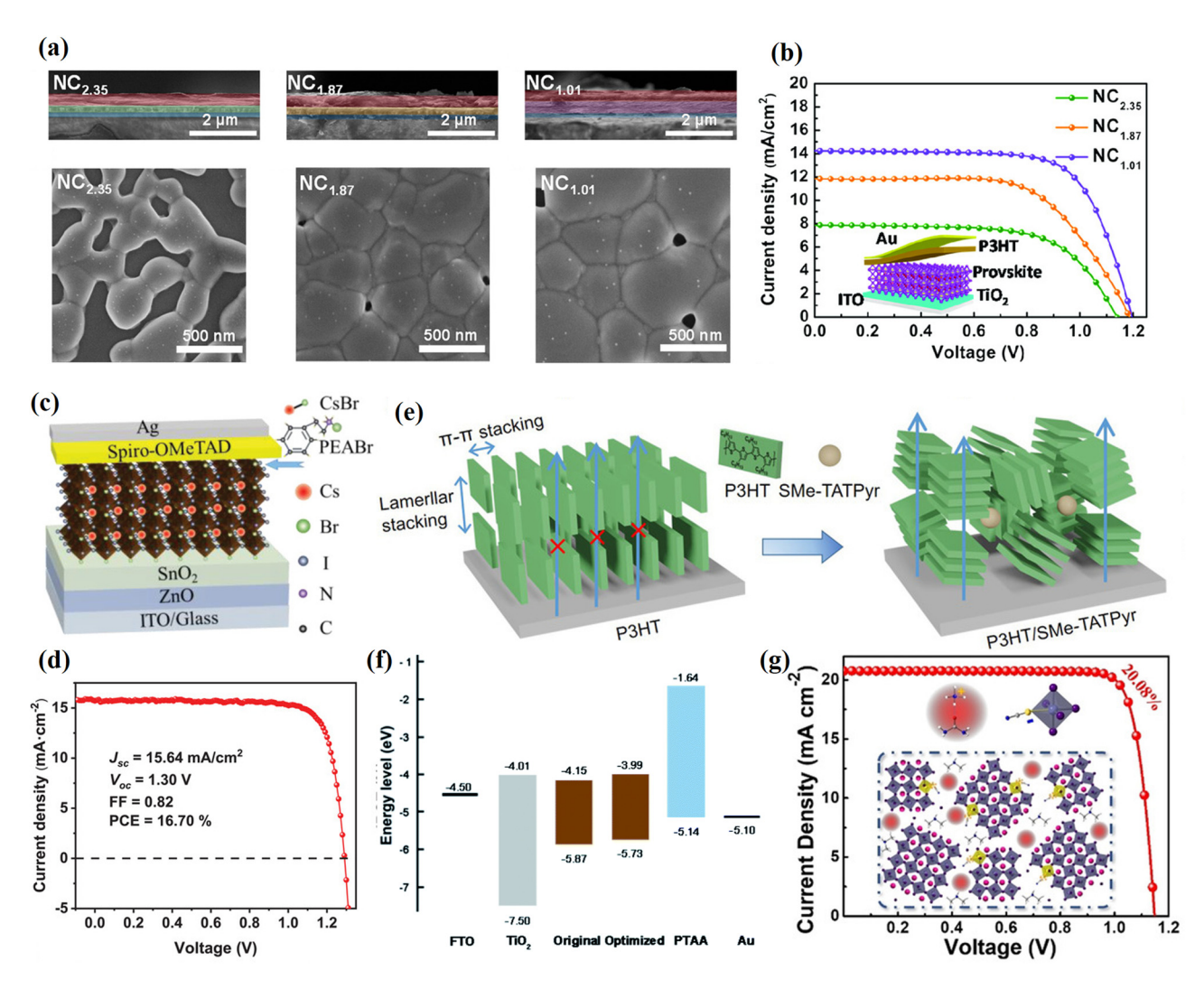


Figure 8: (a) The cross-sectional SEM images of NC_{2.35}, NC_{1.87}, and NC_{1.01} and the SEM images of the annealed CsPbBrl₂ film fabricated by NC_{2.35}, NC_{1.87}, and NC_{1.01}. (b) The reverse scan *J–V* curves of NC_{2.35}, NC_{1.87}, and NC_{1.01}. Reproduced with permission from ref. [98]. Copyright 2020, Wiley-VCH. (c) Structure diagram of the experimental device with the structure of Glass/ITO/ZnO/SnO₂/CsPbl₂Br/(PEABr + CsBr)/Spiro-OMeTAD/Ag. (d) *J–V* characteristic curve of the best device with the optimized PEABr + CsBr. Reproduced with permission from ref. [100]. Copyright 2021, The Authors, published by Wiley-VCH. (e) Structure diagram of the molecular stacking of P3HT and P3HT/SMe-TATPyr, reproduced with permission from ref. [99]. Copyright 2021, Wiley-VCH. (f) The energy band diagram of CsPbl₃ PSCs, reproduced with permission from ref. [102]. Copyright 2020, The Royal Society of Chemistry. (g) *J–V* curve and structure diagram of CsPbl₃ PSC modified by the UAT, reproduced with permission from ref. [103]. Copyright 2021, Wiley-VCH.

16.70%, as shown in Figure 8d. Besides, in order to solve the serious electrical loss problem of PSCs, Li *et al.* designed a small conjugated donor molecule (SMe-TATPyr) to control the accumulation characteristics of P3HT. Figure 8e is a schematic diagram of molecular stacking, showing the destructive effect of SMe-TATPyr on the structure of P3HT and the formation of P3HT clusters, which improves hole mobility. The PCE of the final prepared CsPbI₂Br PSCs was 16.93% [100]. This method effectively improves the moisture stability and thermal stability of PSCs.

All-inorganic perovskite and CsPbI₃ PSCs have attracted more attention due to their superior stability and suitable

band gap. For all-inorganic perovskites, Wu *et al.* invented an all-inorganic perovskite/organic tandem solar cell, in which the top cell is CsPbI_{2.1}Br_{0.9} with a wide band gap, and the bottom cell is an organic photosensitive layer (PM6:Y6) with a narrow band gap [101]. This solar cell can finally obtain a PCE of 18.06%, which is one of the highest efficiencies of all-inorganic/organic tandem solar cells currently reported. For CsPbI₃ PSCs, Yan *et al.* prepared efficient CsPbI₃ PSCs by adding guanidine hydrobromide (GABr) to the exterior of the CsPbI₃ film [102]. Figure 8f is the energy band diagram, the optimized maximum PCE is 18.02%, which is higher than the original PCE (16.58%). Through

further research, the characterization of passivation was found, resulting in the decrease in the non-radiative recombination rate. In addition, the energy band arrangement between CsPbI₃ and the interface layer is optimized, reducing the electron transport barrier, providing good hole contact, and ultimately hindering the flow of electrons in the opposite direction. Furthermore, Yu *et al.* also optimized the crystal of the CsPbI₃ film and added a new type of urea-ammonium thiocyanate (UAT) molten salt as an additive for all-inorganic cesium triiodide lead solar cells, which obtained a PCE of up to 20.08% with excellent stability, as shown in Figure 8g [103]. Specifically, it is to utilize and release the coordination activity of SCN⁻ as much as possible to deposit high-quality CsPbI₃ film.

Light immersion can improve the performance indicators of PSCs, but the unstable output power will cause damage during the period. In this regard, based on the discovery that light immersion can promote the migration of halide ions, Wu *et al.* proposed that the CsPb(Br_xI_{1-x})₃ precursor solution was doped with slightly higher stoichiometric PbI₂, and finally obtained a PCE as high as 18.14% [104].

In short, new and stable charge transport materials, additives, and doping concentrations are the direction for future research on the efficiency and stability of PSCs. In particular, inorganic PSCs can effectively solve the problem of low stability of organic PSCs, but the PCE still needs to be continuously improved.

3.2 Decryption and encryption of information

Perovskite crystals can be used to decrypt and encrypt confidential information. Zhang *et al.* found that traditional smart fluorescent materials are visible under UV light or ambient light, which may damage the protection of confidential information [6]. Therefore, they proposed a method to protect and store confidential information by converting lead-based MOF into luminescent perovskite NC and used lead-based MOF powder to prepare CH₃NH₃PbBr₃ (MAPbBr₃) NCs, as shown in Figure 9a. The invisibility and controllable printing characteristics of lead-based MOF can

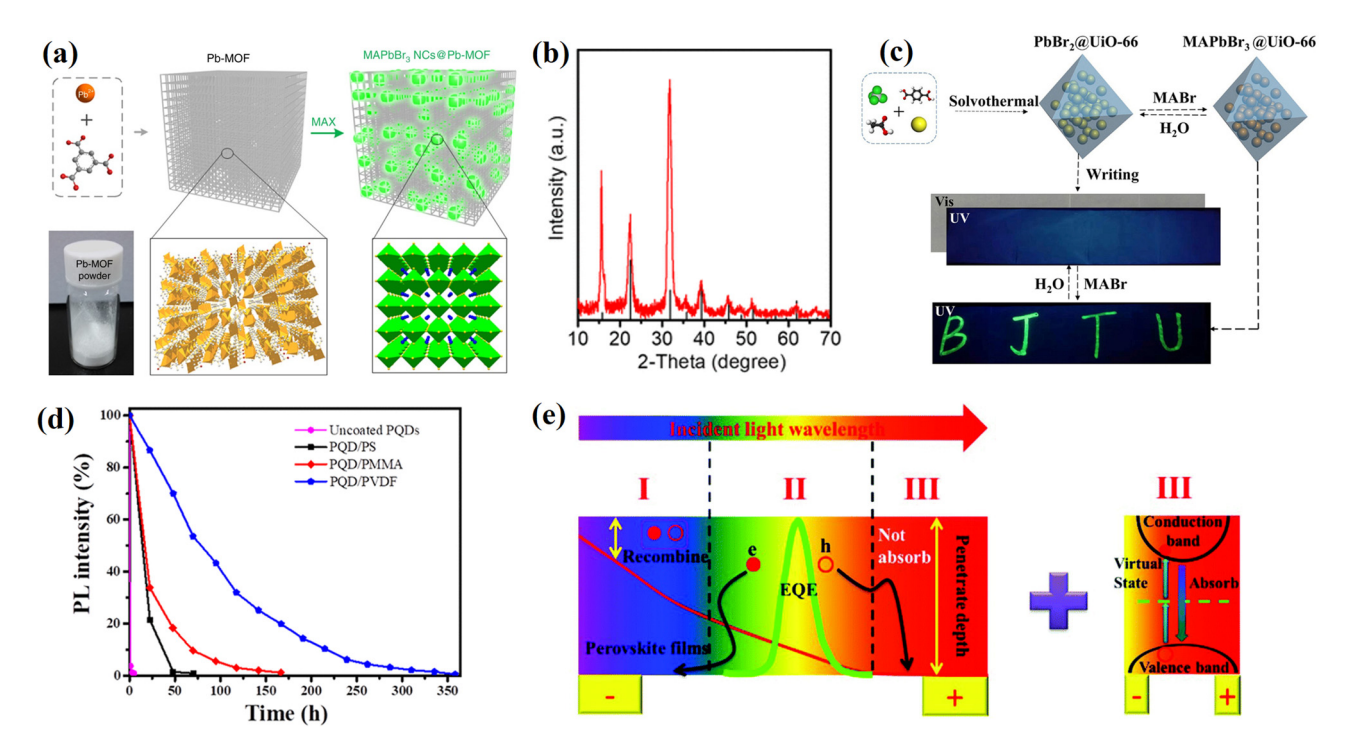


Figure 9: (a) Schematic diagram of the conversion of lead-based MOF powder to CH₃NH₃PbBr₃ (MAPbBr₃) NCs, reproduced with permission from ref. [6]. Copyright 2017, The Author(s), published by Springer Nature. (b) XRD pattern of CsPbCl₃ QDs, reproduced with permission from ref. [7]. Copyright 2019, American Chemical Society. (c) Reversible fluorescence conversion characteristics and application in optical information protection of MAPbBr₃@UiO-66, reproduced with permission from ref. [105]. Copyright 2020, Elsevier. (d) PL intensity of the uncoated PQDs, PQD/PS, PQD/PMMA, and PQD/PVDF, reproduced with permission from ref. [106]. Copyright 2020, American Chemical Society. (e) Schematic diagram of a highly narrow-band PD and TPA PD based on inorganic halide perovskite, reproduced with permission from ref. [107]. Copyright 2018, The Royal Society of Chemistry.

record and encrypt confidential information through the MOF mode. However, common decryption methods cannot read confidential information. Only by using polar solvents (such as methanol) and halide salts to react with MOF can the high-luminescence perovskite NC be quickly and simply formed, thereby promoting effective information decryption.

For information security applications, fluorescent ink has become the most convenient way to be used due to its convenience and low cost. However, the PL characteristic of fluorescent ink makes it usually visible under ambient light or UV light, so there is still the possibility of information leakage. In this regard, Sun et al. used the fullcolor stimulus-response ink based on high PLQY, bright PL, ion exchange reaction, and wide color gamut PQDs to encrypt and decrypt information [7]. Figure 9b is the data after X-ray diffraction (XRD) measurement of the crystal structure of CsPbCl₃ QDs. The average particle size of 10 nm can be obtained by calculation. Using butylamine and acetic acid as reagents to turn off and turn on the light, thereby encrypting and decrypting the printed information. The information made by the halide salt solution can only be read under UV light after spraying with a specific developer and has high stability. It can be stored for several decades at most, and it can be stored for several weeks even after decryption.

In addition, MAPbBr₃ perovskite has attracted widespread attention because of its high PLQY and tunable PL advantages. MAPbBr3 exhibits poor stability and low visibility under UV light and ambient light, so Shi et al. combined PbBr2, MAPbBr3 based on Zr-based MOF UiO-66 [105]. Figure 9c shows the reversible fluorescence conversion characteristics and application in optical information protection of MAPbBr₃@UiO-66. PbBr₂@UiO-66 was converted to luminous MAPbBr₃@UiO-66 to prepare stable PbBr₂@UiO-66 and luminous MAPbBr₃@UiO-66 composite materials, realizing information encryption and decryption. Since PbBr₂@UiO-66 is invisible under ambient light and UV light, the information can be recorded and encrypted, and ordinary decryption methods cannot read this information. Using the MABr solution that reacts with PbBr₂@UiO-66 can quickly form high-brightness MAPbBr₃@UiO-66 in situ, thereby facilitating information decryption. Finally, through water and MABr solution treatment, the luminescence of MAPbBr₃@UiO-66 can be quenched and restored for the encryption and decryption of multiple information.

In optical multiplexing, using the time dimension is an effective way to improve the security of data encryption. Unfortunately, adjusting the fluorescence lifetime of a luminescent material usually changes its fluorescence spectrum, which is not conducive to the protection of confidential information. Therefore, Liu et al. prepared an ideal multi-dimensional data encryption material, which has a long and adjustable fluorescence lifetime but the same fluorescence spectrum as various perovskite QDs/polymer nanospheres [106]. Figure 9d is the PL intensity of the uncoated PQDs, PQD/PS, PQD/poly(methyl methacrylate) (PMMA), and PQD/poly(vinylidene fluoride) (PVDF). As can be seen in the figure, the stability of the three PQD/polymers has been improved, but the stability of PQD/PVDF is significantly higher than the other two. This data encryption strategy takes advantage of the water sensitivity of perovskite and the water stability between uncoated perovskite QDs and PQDs/polymer to realize the spatial dimension encryption of information. In order to realize the time dimension data encryption, the fluorescence lifetime of the PQDs/polymer is used as a coding element. The data are decrypted by fluorescence lifetime imaging microscope and time-controlled luminescence imaging technology.

In optical communication, the openness of the optical channel greatly weakens the confidentiality and security of information. Therefore, Wu *et al.* developed a visible light-infrared dual-mode narrow-band perovskite PD and proposed to use the two advantages of narrowband and two-photon absorption (TPA) to encrypt the optical communication of the PD [107]. Figure 9e is the schematic diagram of a highly narrow-band PD and TPA PD based on inorganic halide perovskite. When the 532 nm and 442 nm lasers are used to send information and noise signals at the same time, the perovskite PD only receives the main information. However, the commercial Si PDs respond to both types of light, resulting in the loss of the main information. The final data only can be predetermined by the key through the TPA process.

In short, the use of perovskite materials can be used to realize the protection of advanced encrypted information, and it will occupy an important position in the fields of future secure communication and information anticounterfeiting. However, PQDs contain toxic Pb elements. In the future, how to reduce Pb elements or find alternative elements will be an important research direction. Solving this problem will help it further expand the scope of application.

3.3 VLCs

In the last decades of the 20th century and the beginning of the 21st century, wireless communication technology

developed rapidly and became popular, playing a pivotal role in the communication industry. However, the capacity of the electromagnetic spectrum used by the wireless system has a limited capacity, and the license to use a part of the spectrum is expensive. With the rise in the large amount of data wireless communication, the shortage of radio frequency (RF) spectrum resources makes companies consider choosing to use UV visible spectrum instead of RF. In recent years, wireless optical communication technology based on visible light has begun to become a research hotspot in academia. VLC is a kind of environmentally friendly information technology that uses light transmitters (such as LEDs, LD light sources, etc.) to transmit signals and light receivers (such as PIN, avalanche photodiodes, etc.) to receive signals. It can transmit in free space or underwater to establish a wireless optical communication link between the receiver and the transmitter. The development momentum of VLC mainly includes the following aspects: i) A higher frequency, about 10,000 times the radio frequency, and a higher bandwidth, ii) No impact on WiFi and RF networks, iii) No harm to human health, and iv) Lower power and cost than RF [108-111]. Compared with other popular wireless technologies (such as Bluetooth, WiFi, and IrDa), VLC possesses higher data density and transmission speed (>10 Gbps in an indoor system of several meters) [112]. VLC has broad application prospects and can be used anywhere as a communication medium for computing, television, traffic signs, payment cards [113], indoor positioning systems [114], wireless local area networks, and vehicle networks.

In recent years, LEDs made of perovskite materials have made great progress [115-117], especially the external quantum efficiency (EQE) of green and red emission has reached more than 20% [79,118]. However, it is difficult to synthesize stable materials in the form of thin films while maintaining high quantum efficiency, resulting in the EQE of blue emission being still low [119]. Therefore, Chu et al. developed a perovskite film with a blue PLOY greater than 70% [63]. The main method is to introduce large cation CH₃CH₂NH₂⁺ (EA) into the Cs⁺ site of PEA₂(CsPbBr₃)₂PbBr₄ perovskite, as shown in Figure 10a, and adjust the emission from green (508 nm) to blue (466 nm). Under light and heating conditions, the blue emission has good spectral stability, as shown in Figure 10b. The 12.1% EQE sky blue (488 nm) electroluminescence (EL) obtained will benefit the future development of Perovskite LEDs (PeLEDs) in the field of full-color displays.

In addition, Pang et al. proposed a method for realizing a high-efficiency sky blue PeLED by adjusting the low-dimensional phase distribution in the quasi-2D perovskite [8]. The main method of this sky blue perovskite LED is to add Na⁺ to the quasi-2D perovskite mixed with Cl/Br, cesium lead halide as the inorganic framework, and phenylethylamine as the organic spacer. By adjusting the phase distribution, a stable 11.7% maximum EQE is achieved.

LEDs based on PQDs (QLEDs), which are materials for high-quality luminescence and display, have the characteristics of a wide color gamut and true-color performance. However, the QD film caused a large number of defects during the assembly process, which greatly reduced the performance of the QLEDs. In optoelectronic devices, the perovskite layer is usually located in the center of the sandwich structure. Both the top and bottom surfaces of the film face interfacial problems, and defects and partially deposited material can affect carrier motion. Therefore, Xu et al. proposed a double-sided passivation method to evaporate a layer of organic molecules between the QD film and the carrier transport layer (CTL). The interfaces between the bottom and top of the QD film and the organic molecules are passivated. Due to the strong interaction of perovskite and the blocking between perovskite and CTL, the stability of perovskite OLEDs is effectively improved [9]. Figure 10c is a device structure diagram and a cross-sectional TEM image of a double-sided passivation device. Finally, the EQE can reach 18.7%, as shown in Figure 10d, the current efficiency is 75 cd⁻¹ and the service life was increased to 15.8 h.

Research has found that liquid perovskite QDs (LPQDs) have more excellent characteristics than solid perovskite QDs (SPQDs). Liang et al. synthesized CsPbBr3 perovskite QDs with ultrasound, finding that LPQDs have a shorter luminescence lifetime of 24 ns shorter than SPQDs [22]. In order to make full use of this excellent feature of LPQDs, they applied LPQDs as color converters to construct LDbased white light systems for implementing VLC for the first time, as shown in Figure 10e, finding a data transmission rate of up to 1 Gbps. According to the bandwidth measurement in Figure 10f, the bandwidth of LPQDs is nearly 30% higher than that of SPQDs. This experiment proves the wide application of LPQDs in VLC.

A high-bandwidth system combining blue LED and PQDs has also been proposed previously. Mei et al. designed a new VLC all-inorganic white light device, which uses blue gallium nitride (GaN) micro-size LED (µLED) as the light source and inorganic yellow light-emitting perovskite CsPbBr_{1.8}I_{1.2} QDs (YQDs) as the color converter [120]. The 2D structure diagram of the fabricated µLED is shown in Figure 11a. Figure 11b is an experimental device designed to test the communication performance of a white light system. Using the non-return-to-zero keying (NRZ-OOK) modulation method, the maximum data transmission rate of 300 Mbps can be obtained. Combining µLED and

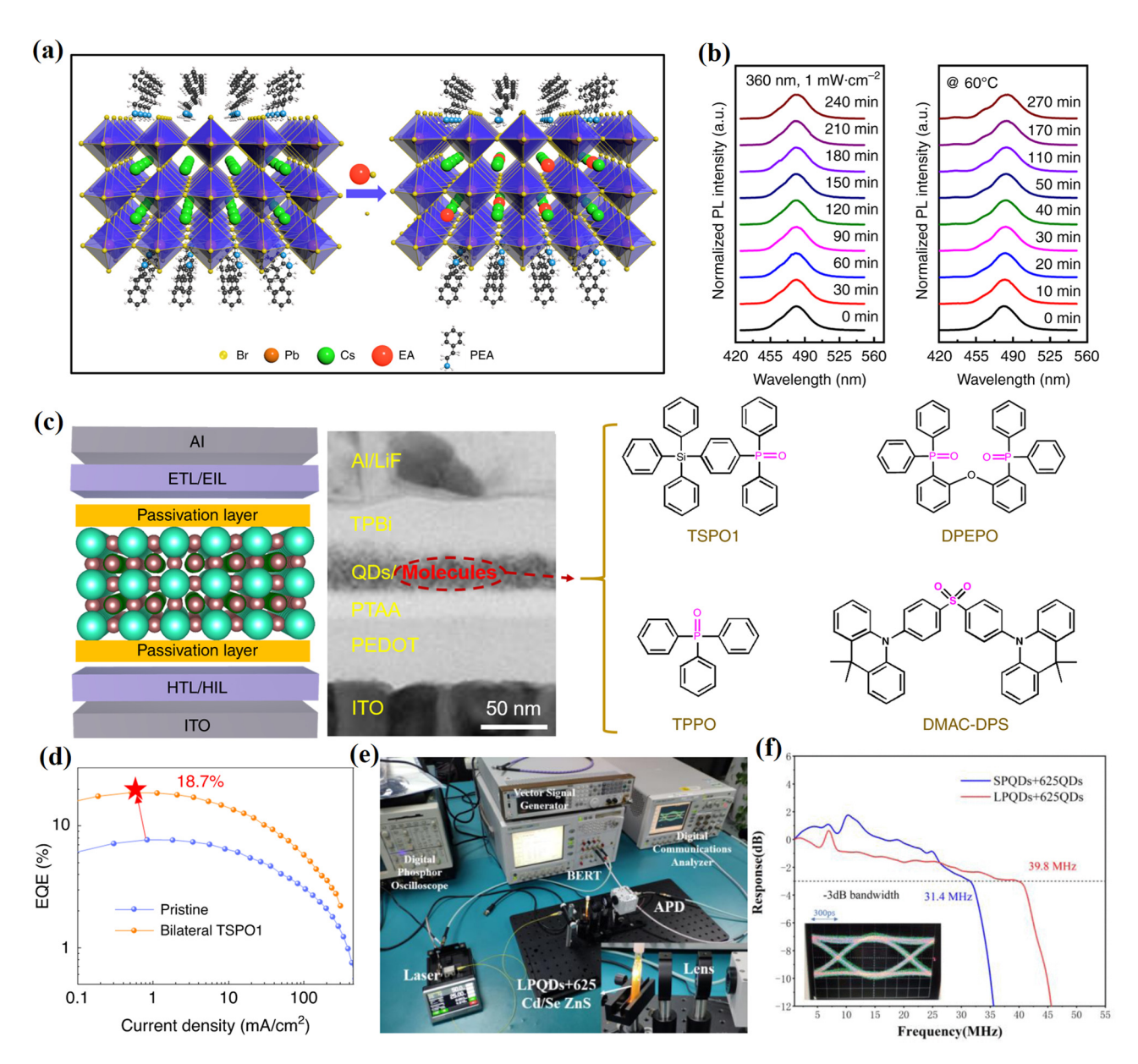


Figure 10: (a) Structure diagram of EA cation in perovskite lattice replacing Cs⁺ in quasi-2D perovskite. (b) Normalized PL spectrum of quasi-2D perovskite film with 60% EABr content after continuous UV radiation and continuous heat treatment. Reproduced with permission from ref. [63]. Copyright 2020, The Authors, published by Springer Nature. (c) The device structure diagram and cross-sectional TEM image of the bilateral passivation, the passivation molecules are TSPO1, DPEPO, TPPO, and DMAC-DPS, respectively. (d) EQE of the pristine and bilateral-passivated devices. Reproduced with permission from ref. [9]. Copyright 2020, The Authors, published by Springer Nature. (e) VLC system based on LD. (f) Bandwidth measurement of white light illumination system based on LD. Reproduced with permission from ref. [22]. Copyright 2019, IEEE.

perovskite QDs, the maximum -3 dB electrical-to-optical (E-O) modulation bandwidth is about 85 MHz, as shown in Figure 11c. In addition, the bandwidth of the white light device and YQDs has no obvious attenuation, which fully demonstrates its high stability.

In order to further increase the data transmission rate, Leitão *et al.* used a brand new inorganic perovskite QD (IPQDs) material to develop a color converter optical

pump based on 450 nm InGaN LED, which can be used for VLC [121]. Only the light after color conversion can be used as the signal optical carrier of this experiment, which can achieve 364 Mbps free space data communication. When mixed with unabsorbed LED light, the data rate will exceed 1 Gbps and it will also be displayed.

For the development of the visible light integration platform, Trofimov *et al.* developed a visible light platform

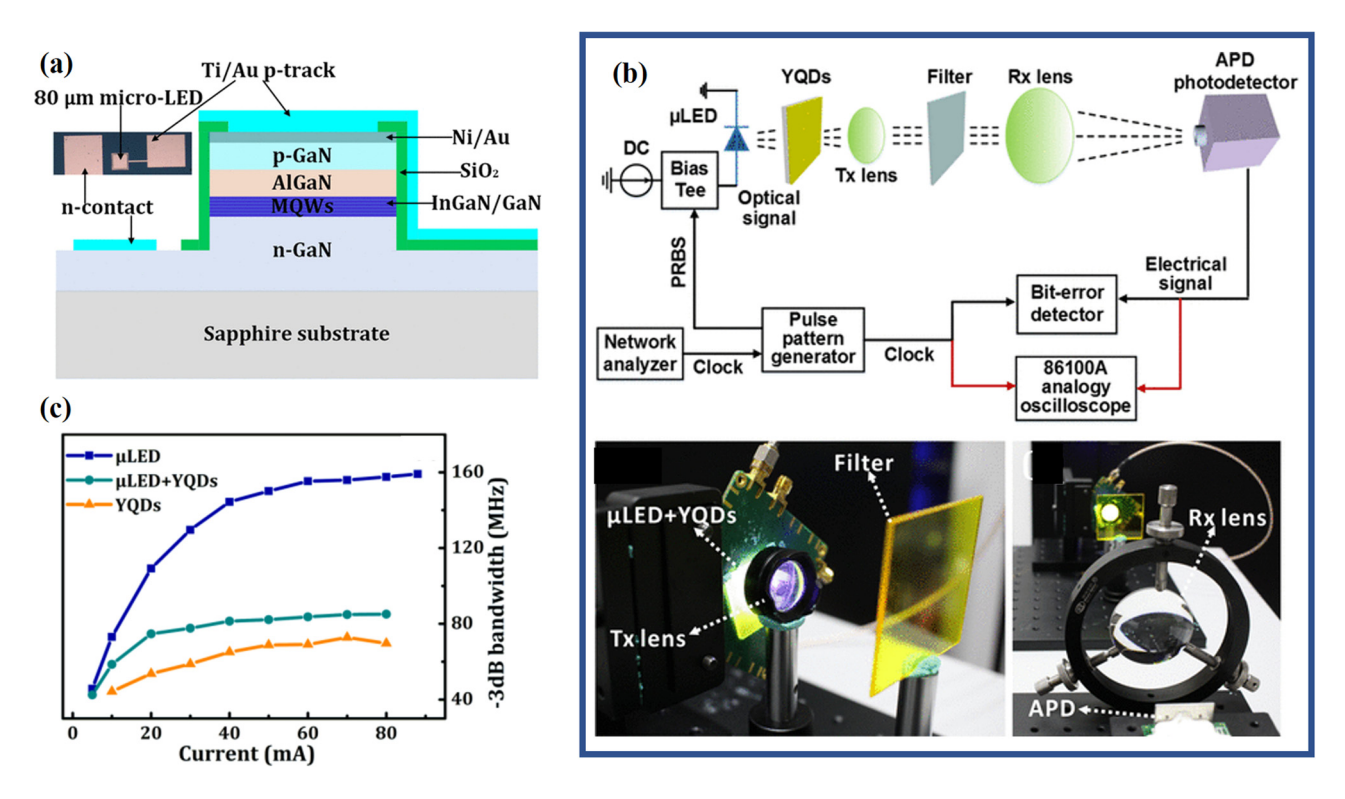


Figure 11: (a) 2D structure diagram of the fabricated μLED. (b) VLC link diagram and experimental device. (c) Comparison of -3 dB modulation bandwidth between μLED, μLED + YQDs system, and YQDs. Reproduced with permission from ref. [120]. Copyright 2018, American Chemical Society.

based on a spectrally tunable perovskite (CsPbX₃) microscale light source and series low-loss 3D semiconductor GaP nano-waveguides [122]. In this device, the perovskite microcrystalline core supports a stable room temperature laser, and the tuning range of the broadband chemical emission wavelength is 530–680 nm. The GaP nano-waveguide supports high-efficiency light outcoupling, and its sub-wavelength is <200 nm limitation and long-distance guiding distance exceeds 20 μ m.

PDs are the basis for optical communication and biosensing applications, which can convert an optical signal into an electrical signal. Unfortunately, there are problems such as crosstalk, interference, and data leakage in VLC, so higher requirements are placed on the PD and the receiving end in terms of fast and accurate signal identification and fast decoding. In this regard, Huang *et al.* proposed a dual-frequency PD based on MAPbBr₃ and MAPbI₃ as the photoactive layer, and superimposed two photodiodes with opposite polarities as the effective receiving end of the VLC [123]. By controlling the direction of the bias voltage, the response of the device can be switched between 300 and 570 nm and between 630 and 800 nm, the optical crosstalk is less than -30 dB, and the detection performance is 1.75×10^{10} Jones. The device can

efficiently detect signals of different wavelengths from commercial white LED (WLED) transmitters, allowing simple encryption at the receiving end in VLC, reducing the potential for message leakage. To further expand the spectral response range and improve the EQE of perovskite PDs, Wang et al. prepared highly sensitive perovskite PDs with an active layer of (FASnI₃)_{0.6}(MAPbI₃)_{0.4} [124]. When the thickness of (FASnI₃)_{0.6}(MAPbI₃)_{0.4} is 1,000 nm and the thickness of the C₆₀ layer is 70 nm, the spectral response range of PDs is extended to the near-infrared region, and the EQE value exceeds 65%. Miao and Zhang reviewed the latest progress and specific methods on how to expand the spectral response range of perovskite PDs and improve various performance indicators [125]. At the same time, promising directions such as multifunctional perovskite PDs and flexible transparent perovskite PDs are also proposed. Tong et al. combined CH3NH3PbI3 and dioctylbenzothieno [2,3-b] benzothiophene (C8BTBT) to construct PDs with perovskite/organic heterostructures, which work in the UV to near-infrared region, with a fast response time of 4.0 ms and a high $I_{\text{light}}/I_{\text{dark}}$ of 2.4 × 10⁴ [126]. In addition, Zhou et al. proposed a perovskite PDs with high detection of $\sim 10^{13}$ Jones and responsivity of 10⁵ A W⁻¹ at 360 nm, composed of graphene-poly[bis(4-phenyl)(2,4,6-trimethylphenyl)amine]

(PTAA)-perovskite-poly(methyl methacrylate) (PMMA) [127].

In a VLC system, fast response and highly sensitive detectors are also indispensable. Ma et al. used organic/inorganic hybrid perovskite (CH₃NH₃PbI₃) to prepare a PD with a fast response time and high response rate by improving the quality of the photosensitive layer and selecting the appropriate transport layer [128]. Figure 12a and b are the schematic diagram and physical image of the VLC system based on the organic/inorganic hybrid perovskite PD, and Figure 12c is the text data waveform received by the detector. Under zero bias conditions, the device has a high response rate of 436 mA W $^{-1}$ at 753 nm, a fast response time of 1.7 μ s, a linear dynamic range of 106 dB, and a bandwidth of 75 kHz. Based on the abovementioned remarkable characteristics, the perovskite PD can be integrated into an optical communication system as a receiving end optical sensor, and can quickly, successfully, and accurately transmit character strings, texts, and data files through optical coding.

The traditional fluorescent solid-state lighting (SSL) in VLC is composed of wide-area LEDs that emit blue light and phosphors that emit yellow light. However, the E–O modulation bandwidth of the phosphor is very low, which limits the data communication rate to a certain extent. Therefore, we need to find a color converter with higher bandwidth to increase the communication rate. QDs also have the characteristics of the tunable emission spectrum, narrow emission spectrum, and high QY, so they have

become popular SSL conversion materials. In addition, QDs can achieve a high data transmission rate and modulation bandwidth within a few nanoseconds or even tens of nanoseconds due to their short fluorescence lifetime. For example, Xiao *et al.* proposed a light conversion material based on CdSe/ZnS QDs and related luminescent microspheres as QD-LEDs [129]. The modulation bandwidth of the proposed QD-LED and QD-WLED was increased by 74.19% and 67.75%.

At present, silicon (Si) PDs have become basic components and are widely used in optoelectronic devices. These devices are based on their broadband spectral response, ultra-high response rate, high reliability, and mature low-cost manufacturing process. But the UV light response of Si PDs is relatively low due to the limitation of high reflection coefficient and light penetration depth. Ding et al. perfected the thermal injection method to prepare Cr³⁺, Yb³⁺, Ce³⁺ triple-doped CsPbCl₃ PQDs [130]. The 188% PLQYs and excellent stability confirm the extremely efficient UV-NIR quantum cutting emission, which greatly improves the effectiveness of the UV response of Si PDs. This is mainly due to the enhanced exciton binding. Doping Cr³⁺ can reduce energy, reduce defects, and improve tolerance coefficients. At the same time, Ce³⁺ is used to increase the bridge coefficient, which improves the energy transfer from PQD to Yb3+. In addition, the 5d high energy state of Ce³⁺ ion significantly enhances the UV absorption of PQDs. A full spectrum response of

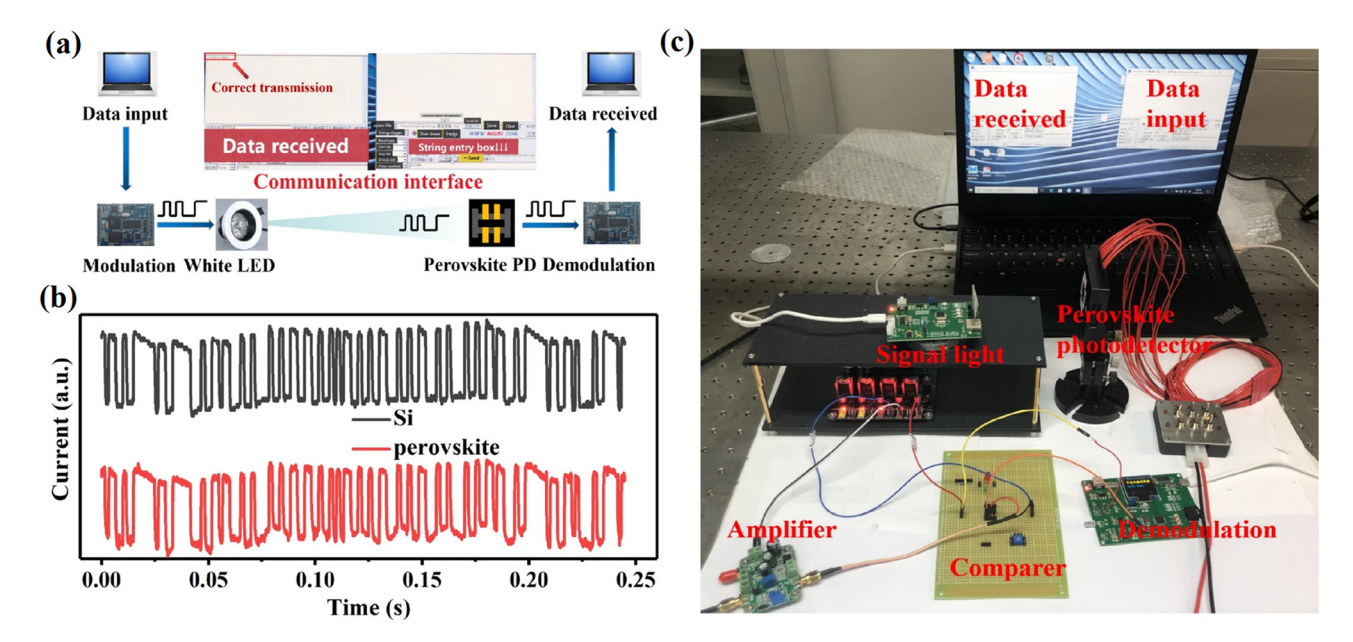


Figure 12: (a) Schematic diagram of VLC with perovskite as the PD. (b) Text data waveform received by perovskite PD. (c) Experimental setup of the VLC system based on organic/inorganic hybrid perovskite PD. Reproduced with permission from ref. [128]. Copyright 2020, Springer Nature.

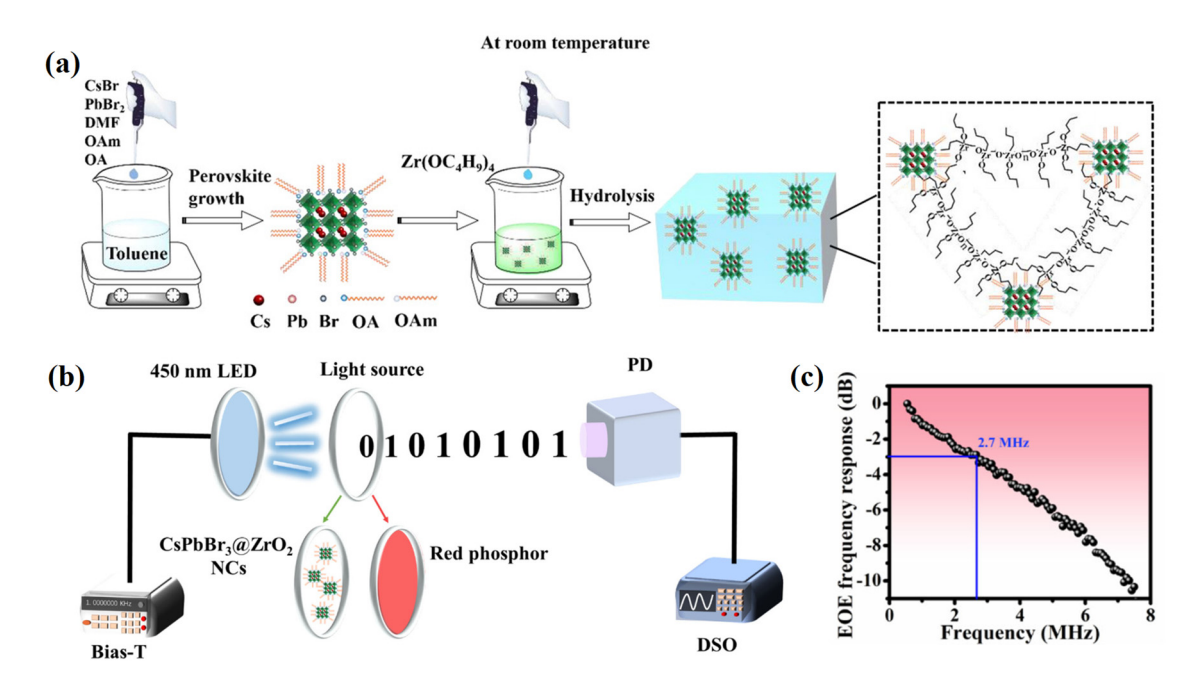


Figure 13: (a) Preparation process of CsPbBr₃@ZrO₂ NCs. (b) Schematic diagram and (c) frequency response of the VLC system. Reproduced with permission from ref. [132]. Copyright 2021, Wiley-VCH.

200–1,100 nm is achieved with excellent stability by the integration of Si PDs and PQDs.

It is well known that efficient UV light detection methods are also an important means to promote the development of UV light communication. Kang *et al.* proposed a hybrid Si-based light detection scheme [131]. The solution uses CsPbBr₃ perovskite NCs with high PLQY and fast PL decay time, which can be used as an UV-visible color conversion layer for high-speed solar-blind UV communication. Compared with commercial silicon-based PDs, the response rate of the solar-blind zone has increased by nearly three times, and the EQE has increased by about 25%.

In order to solve the problem of poor stability of CsPbBr₃ NCs, Mo *et al.* proposed a simple method to synthesize CsPbBr₃@ZrO₂ NCs in the air at room temperature, which only takes 20 s, as shown in Figure 13a [132]. They also combined CsPbBr₃@ZrO₂ NCs with blue InGaN chips to prepare WLEDs. The prepared high-performance WLED is applied to the VLC system (Figure 13b) to achieve a -3 dB bandwidth of 2.75 MHz (Figure 13c) and a communication rate of 33.5 Mbps.

For PDs with a wide range of applications, Hu *et al.* developed a high-performance broadband heterojunction PD [133]. Because the perovskite film designed on the single crystal germanium layer is uniform and pinhole-free, the perovskite/germanium PD has a stronger performance and wider spectrum. In the photon response

characteristics, when the optical fiber communication wavelength is 1,550 nm, the highest response rate of the heterojunction device is $1.4~\mathrm{A~W^{-1}}$, the thickness of the telecommunication band is optimized to 150 nm, and the performance is significantly improved. At the visible wavelength of 680 nm, the response rate of the device is 228 A W⁻¹, and the detection rate is $1.6~\times~10^{10}$ Jones. Based on this germanium/perovskite heterostructure configuration, it provides a new foundation for new optoelectronic devices.

In short, perovskite materials can be used for both light emitters and light receivers. It is a promising material for high-speed VLC in the future and has made great progress. In particular, inorganic perovskite materials have extremely short response times, extremely high stability, and simple manufacturing. They have great potential in affecting the development of VLC.

3.4 Optical neuromorphic devices for photonic synapse and photonic neural calculation

As we can see from the previous sections, the industry has mastered the technology of preparing metal hybrid perovskite by solution method, which is the most mainstream preparation method at present. Meanwhile,

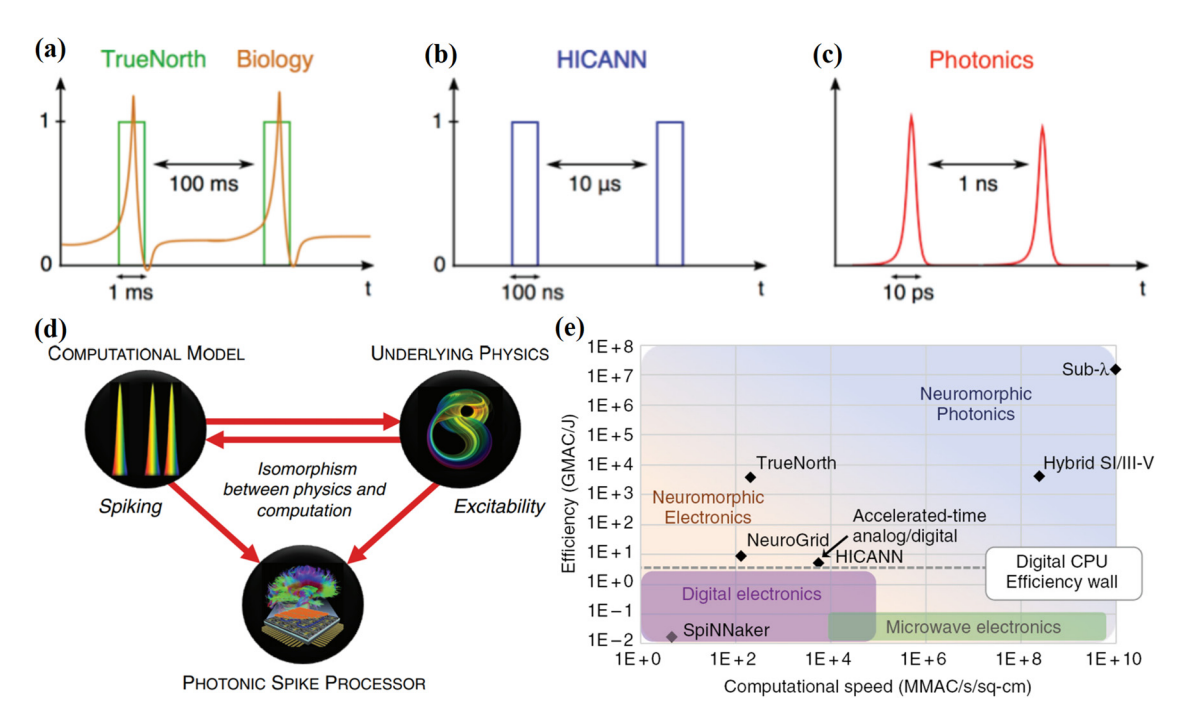


Figure 14: The physical time scales of (a) biological neurons, (b) electronic spiking neurons, and (c) photonic neurons. (d) Photonic spiking processor for optical computing analogies. Reproduced with permission from ref. [134]. Copyright 2017, Taylor & Francis Group. (e) Computational speed and efficiency metrics of various neuromorphic hardware platforms, reproduced with permission [135]. Copyright 2017, Thomas Ferreira de Lima et al., published by De Gruyter.

perovskite has been diffusely used in optical communications, information encryption and decryption, third-generation solar cells, and other fields due to its excellent optical and electrical properties, which have been discovered by researchers. However, few reviews have investigated and studied photonic memristors made of perovskite materials for optical computing. Compared with electrical computing, optical computing uses photons instead of electrons for computing, which can overcome the inherent limitations of electronics and increase energy efficiency, processing speed, and computing throughput, as shown in Figure 14. Figure 14a-c shows the difference in time scales between biological neurons (Figure 14a), electronic spiking neurons (Figure 14b), and photonic neurons (Figure 14c), which exhibit many orders of magnitude faster than their biological counterparts. Furthermore, the acceleration factors of time resolution and processing speed are close to 100 million [134]. A photonic spiking processor for optical computing is shown in Figure 14d. By reducing the abstraction between process (spikes) and physics (excitability), significant advantages can be obtained in terms of speed, energy usage, and scalability. Figure 14e shows the comparisons of computational speed and efficiency metrics among various neuromorphic hardware platforms [135]. It can be seen that neuromorphic photonics exhibit excellent performances.

Advanced photonic memristors based on perovskite materials are a dynamic and promising field, especially photonic memristive devices based on the excellent luminescence properties of perovskite, which will become the focus of future research in the optical memristor field for photonic synapse, optical computing, light accelerated learning, and so on. It will promote the development of artificial intelligence and make further progress in all optical artificial neural networks. In this section, we give a concise overview of perovskite optical memristors as well as photonic morphology calculation based on perovskites, and make a reasonable prospect for their future development.

3.4.1 Optical neuromorphic devices based on perovskite materials

Generally, optical neuromorphic devices based on perovskite materials can be mainly divided into two categories: two-terminal memristors and three-terminal transistors. Therefore, we will investigate the research progress of two-terminal and three-terminal optical neuromorphic devices based on perovskite materials in this chapter.

In 1971, when Leon Chua studied the relationship between charge, current, voltage, and magnetic flux, he first proposed the concept of the fourth type of passive device memristor [136]. Due to a lack of empirical evidence, the relevant theory has not attracted attention in the past few decades, until General Electric Research (GER) laboratory Hickmott first reported resistance switch characteristics of the aluminum/alumina/aluminum structure in the 1960s [137]. In the report and study before 2008, most memristors have the mega-ohm resistor sandwich structure using the same metal as a top and bottom electrode. The research on the intermediate function layer focused on the complex perovskite metal oxide [138]. However, the enthusiasm of the researchers for the materials has

waned due to complex processing and compatibility issues. In recent years, with the appearance of perovskite halides with simple process and strong compatibility, coupled with their excellent optical properties, the research of perovskite-based photo-memristor has been put on the schedule.

A photonic flash memory based on all-inorganic PQDs was demonstrated by Wang *et al.* [10] The optical programmable and electrical erasable properties of the implement are based on the heterostructure formed between the CsPbBr₃ QDs and the semiconductor layer (Pentacene/PMMA/CsPbBr₃). Figure 15a is a schematic diagram of synapse structure and artificial synaptic device based on

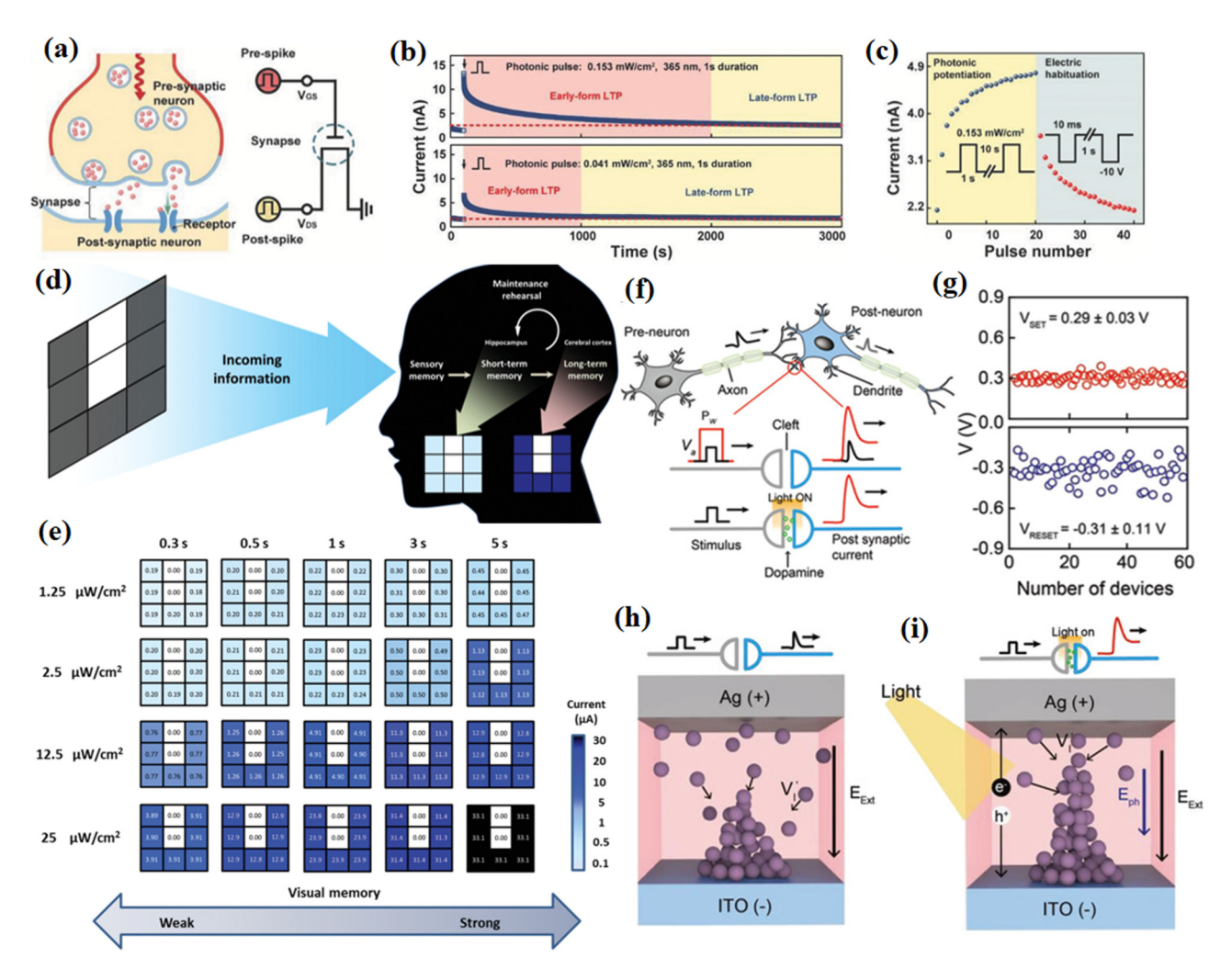


Figure 15: (a) Schematic diagram of synapse structure and artificial synaptic device. (b) Presynaptic application of 365 nm photon pulses to achieve EPSCs under light pulses of different intensities. The device is read at 0.2 V. (c) Reliable potentiation-depression functions of CsPbBr₃-based synaptic devices under photonic pulses and negative electric pulses. Reproduced with permission from ref. [10]. Copyright 2018, Wiley-VCH. (d) Learning and memory models of short-term and long-term memory in the human brain. (e) The letter "U" composed of 3×3 pixels and coded according to different light intensities and light times. Reproduced with permission from ref. [11]. Copyright 2021, Wiley-VCH. (f) Schematic diagram of the synaptic cleft connecting the axon of the pre-neuron and the dendrites of the posterior neuron (top) as well as the schematic diagram of the electrical and chemical signals in the synaptic cleft (bottom). (g) Statistical analysis of V_{SET} and V_{RESET} for the OHP synaptic devices. Schematics of the suggested mechanism in the absence (h) and presence (i) of light for the perovskite-based photonic memristor. Reproduced with permission from ref. [139]. Copyright 2019, Wiley-VCH.

CsPbBr₃ QDs. In addition, this device not only successfully simulates the characteristics of photon enhancement and electrical habit but also simulates the phenomena of spikerate-dependent plasticity, long-term plasticity, and shortterm plasticity in synapses by optical modulation. Figure 15b shows the excitatory postsynaptic current (EPSC) of CsPbBr3-based synaptic devices, which simulates the phenomenon of memory decline, confirming that stronger memories can be retained in the brain as long-term memories. Figure 15c displays the reliable potentiation-depression functions of CsPbBr3-based synaptic devices under the photonic pulse (365 nm, 0.153 mW cm⁻², 1 s duration with 10 s interval) and electric pulse (-20 V, 10 ms duration with 1s interval). Yang et al. demonstrated an ITO substrate-based inorganic perovskite photonic artificial synapse with a two-terminal construction, which more closely resembles the structure of biological synapses [11]. Figure 15d is a typical human brain learning and memory model. The new memory will be temporarily encoded into the hippocampus as short-term memory. Figure 15e confirms the dependence of current on light intensity and illumination time in human visual memory simulated by artificial optical synapses. Moreover, the extra charge transfer absorption of TAPC (an organic matter) doped molybdenum oxide membrane gives the device a transparent appearance. The device responds to light by emitting UV light vertically from the substrate, while performing dual-mode operation under UV and red-light irradiation. This device not only achieves high transparency but also high flexibility. These features help to improve the integration of 3D stacked memristors.

In biological nerves, synapses are the interconnecting parts of the axons of the pre-neurons and the dendrites of the posterior neurons, and can be used as transmission channels for converting chemical signals into electrical signals (Figure 15f). To build a device with basic synaptic functions such as short-term potentiation, long-term potentiation (LTP), and long-term depression, Ham et al. demonstrated a photonic memristor founded on double-ended organic lead halide perovskite (OHP) with the structure of Ag/CH₃NH₃PbI₃/ITO [139]. Statistical analysis of the OHP synaptic device is shown in Figure 15g, from which it can be seen that the V_{SET} and V_{RESET} are about 0.29 \pm 0.03 and -0.31 ± 0.11 V, respectively. In addition, the authors investigated the corresponding conductive switching mechanism without (Figure 15h) and with (Figure 15i) light, and the MNIST pattern recognition based on the perovskite-based photonic memristor in detail. Not only that, the threshold of LTP was further reduced when light was exposed to the OHP synaptic device. This increases the number of available intermediate states and reveals the potential mechanism of light influence on the device. Lin *et al.* proposed to extract organic–inorganic hybrid perovskite material and use it as a resistive layer to prepare non-volatile memory, and the device structure was ITO/PEDOT: PSS/organic–inorganic hybrid perovskite/Cu [140]. The device exhibits excellent electrical bistability and a nonvolatile rewritable memory effect. The new special structure enables it to have light response behavior. Using electric field and light as input sources, the device is proved to have the function of electronic memory and optical induction logic circuit.

CsPbBr₃ QDs were applied to memristors and an asymmetric electrode structure of memristors was prepared [141]. This device can be used to create non-volatile memristor functions with photon modulation and integrated synaptic plasticity tailoring behavior. The device can be programmed and erased by the input bias voltage. In addition, the device exhibits synaptic plasticity and sensitivity to low UV light. Yang et al. proposed to apply the ITO/PMMA/PQDs: PMMA/PMMA/Ag structure based on CH₃NH₃PbBr₃ perovskite quantum dots (PQDs) to nonvolatile memory [74]. The preparation process of QD colloidal solution uses the centrifugal method, which makes the perovskite particle size greatly reduced. The PL peak moves from 552 nm to 535 nm, and the full-width half peak of the PL spectrum decreases from 25 nm to 18 nm, resulting in the quantum confinement effect. Meanwhile, the switching current ratio of the device is greater than 10³ with good reproducibility, reliability, and flexibility. The preparation and synthesis method of QDs are also simple and easy.

An all-inorganic non-volatile memory cell was fabricated by using Cs₄PbBr₆ thin film by Cai et al., which was prepared by the low-temperature synthesis method [142]. The device structure was Au/Cs₄PbBr₆/PEDOT:PSS/Pt, and Cs₄PbBr₆ was used as an insulating layer. This novel structure enables the device to have the light response behavior reflected by the resistance state change. The formation and annihilation of the bromide ion vacancy filaments lead to the logical "OR" function of the device, which can be observed by applying bias voltage and illumination as input signals. Zhang et al. used all-inorganic materials to prepare non-volatile resistive random-access memory (RRAM) with the structure of Au/PMMA/PMMA:CsPbBr₃ NCs/PMMA/ITO. The fabricated device exhibits a change in the formless bipolar high and low resistance ratio from 10⁶ to a stable 10 [143]. In the high resistance state and high resistance ratio, the device shows a fast optical response to the light wavelength from 365 nm to 500 nm. that is, the resistance value changes. At a low resistance switching ratio, the starting voltage of the resistance switch can be controlled by illumination. The work shows that the adjustable resistance switch is realized by light irradiation,

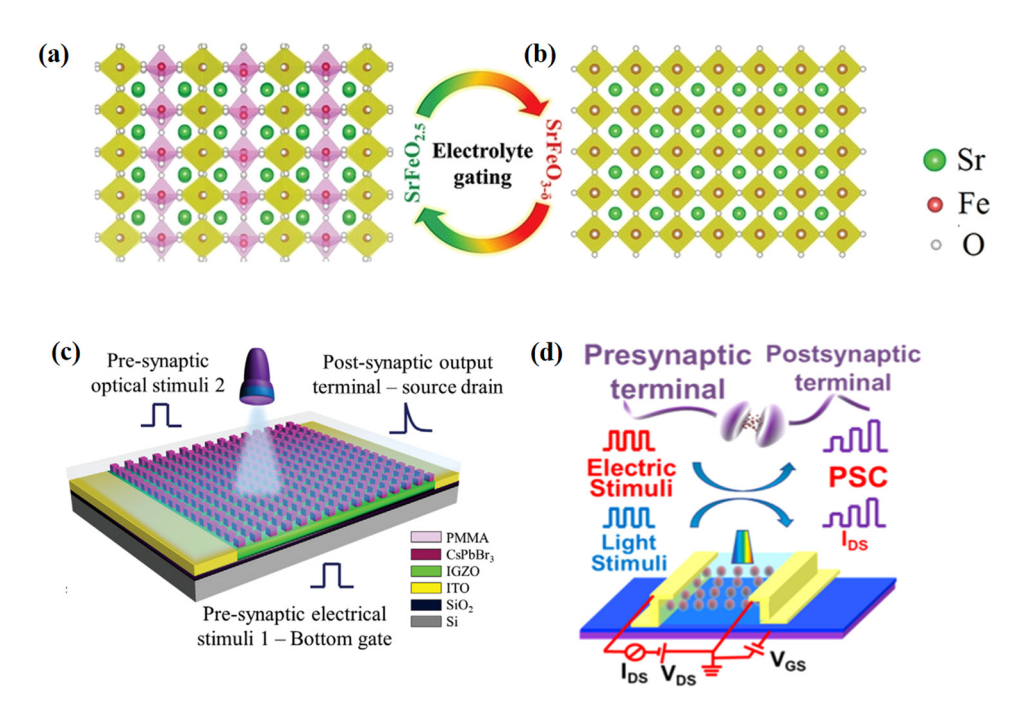


Figure 16: The schematic crystal structures of brownmillerite $SrFeO_{2.5}$ (a) and perovskite $SrFeO_{3-\delta}$ (b) thin films in the $SrTiO_3$ substrate. Reproduced with permission from ref. [144]. Copyright 2019, Wiley-VCH. (c) The proposed multi-gate transistor as artificial synapses. Reproduced with permission from ref. [145]. Copyright 2020, Wiley-VCH. (d) Schematic of emulating a biological synapse by IGZO/perovskite NPs/IGZO TFT. Reproduced with permission from ref. [146]. Copyright 2021, American Chemical Society.

and the light response is embodied by the change in the resistance state.

When it comes to three-terminal neuromorphic devices, a synaptic transistor with ionic-liquid-gated SrFeO_x (SFO) films by exploiting the continuous topotactic phase change reported by GE's group is a good example [144]. Ionicliquid-gated SFO films play an important role in the structure. The structure shown in Figure 16a is responsible for insulation, while conductivity is due to the filling of oxygen atoms (Figure 16b). Because of the good reversibility of the device, the resistive transition is realized by the transformation between the insulating brownmillerite-SFO phase and the conductive perovskite-SFO phase. LTP and long-term depression (LTD) were successfully simulated by applying pulses of different polarities. Symmetric and asymmetric spike-timing-dependent plasticity (STDP) have also been successfully implemented. Besides, the neural network constructed by the device is able to achieve high recognition accuracy.

Periyal with his team fabricated the IGZO/ITO/CsPbBr₃/ PMMA device with a type-II heterostructure, which is formed by spin-coating CsPbBr₃ QDs (≈ 60 nm) on sputtered IGZO (≈ 60 nm) thin films [145]. Figure 16c is the proposed multi-gate transistor as an artificial synapse. The device makes photoelectric programming and decoupling optical absorption and charge transport possible.

Under dark conditions, the devices exhibit typical N-type enhanced mode operation. While being illuminated, the device behaves in depletion mode. By applying a positive (negative) voltage, holes (carrier electrons) move toward the IGZO-CsPbBr₃ interface, resulting in an increase (decrease) in conductivity. The conductance of the device can be adjusted flexibly by the pulse of different parameters, and various synaptic functions can be simulated. Different learning rules can be realized by adjusting the pulse waveform. This is because the wavelength, intensity, and pulse width of optical stimulation all affect the conductance of the device and the weight of the stimulated synapses. Electrical perturbation results in short-term potentiation and, while optical perturbation results in LTP.

Duan *et al.* further fabricated a photo-synaptic thin-film transistor (TFT) based on the IGZO/perovskite (CsPbBr₃) NP composite active layer (Figure 16d) [146]. In aspects of absorbability, perovskite NPs had a broad peak located at ~520 nm. And for perovskite NPs, an emission peak located at 515 nm can be observed in the PL spectrum. Besides, it is reported that more oxygen vacancies ionized in oxide semiconductors can promote the persistent photoconductivity effects and the negative bias illumination stress stability. The device successfully simulates the typical functions of biological synapses. By adjusting the number of pulses, the device can behave as short-term plasticity and long-

term plasticity. Also, paired-pulse facilitation (PPF) phenomena that the second pulse takes much less time than the first to reach the same current can be observed, which is consistent with the law of learning and relearning in the human brain. Compared with pure IGZO devices, the composite TFTs have higher performance and lower power consumption, which is a significant step forward.

3.4.2 Computation of perovskite photonic neural morphology

Inspired by dopamine promoting synaptic behavior, Ham *et al.* designed and fabricated a photonic synapse based on double-ended OHP, in which synaptic plasticity was altered by electrical impulses and light exposure [139]. When the light was applied to the device, the threshold of long-term enhancement was lowered and synaptic weight was further modulated. These factors allow for higher-order tuning of synaptic plasticity, which can accelerate learning at lower power levels in neuro-inspired hardware architectures.

Sun *et al.* demonstrated the plasticity of photoelectric synapses based on 2D lead-free perovskite ((PEA) $_2$ SnI $_4$) and demonstrated several basic synaptic functions of the photoelectric synapses [12]. The intensity of synaptic connections can be effectively modulated by varying the duration, irradiance, and wavelength of the light spikes. In addition, the electrical and optical properties of 2D perovskites can be rapidly modulated through chemical engineering such as composition control, increasing the complexity and freedom required for neuromorphic calculations.

To construct photoelectric synaptic devices, Yin et al. applied the hybrid structure formed by OHP (MAPbI₃) and Si NPs to transistors [13]. The device is very sensitive to light stimulation and can simulate various functions of biological synapses under low-energy consumption light stimulation. Among them, the tunability of EPSC is used to simulate visual learning and memory processes in different emotional states, which is of great significance for the development of silicon-based neuromorphic computation. Hao et al. combined perovskite CsPbBr3 QDs with organic semiconductor materials and applied them in transistors as photonic synapses to realize functions. Synaptic responses include tunable synaptic integration behaviors that implement the "AND" and "OR" optical logic functions [147]. By lighting an array of synapses with different densities of light to change the weight of the synapses, the team successfully simulated an artificial vision system. Ma et al. fabricated photoelectric synapses using all-inorganic perovskite nanosheets and

investigated the plasticity of electronic and photonic synapses, respectively [148]. The device has excellent optical response properties and successfully simulates multifunctional synaptic functions of the nervous system, including pair impulse facilitation, short-term plasticity, long-term plasticity, a transition from short-term to long-term memory, and learning and experiential behavior. In addition, the photoelectric synapse exhibits a unique memory recall function that can extract historical photoelectric information, a detail previously overlooked in this area of research.

A novel neuromorphic optoelectronic device based on a vertical van der Waals heterojunction phototransistor of colloidal OD-CsPbBr₃-QDs/2D-MoS₂ heterojunction channel was proposed by Cheng $et\ al.\ [149]$. The device is photoresponsive and exhibits classical outstanding features such as excitatory postsynaptic current, pairwise impulse facilitation, dynamic time filtering, and phototunable synaptic plasticity. In a simple synaptic network, using synaptic plasticity, the efficiency of tunable photoelectronic Pavlovian associative learning and photoelectronic hybrid neuron encoding behavior were successfully realized by the photoelectric collaboration method.

By growing PQDs directly from the graphene lattice, Pradhan *et al.* prepared G-PQDs superstructure materials, which compensated for the weak charge transfer performance of PQDs [29]. The synaptic function was successfully realized in the photoelectric transistor. The experiment proved that after machine learning, the photon synapse successfully realized the facial recognition function through neural network calculation.

In Table 2, we have a summary of the optical memristive devices based on perovskites. From what has been discussed above, it can be seen that photonic memristor and neural morphology calculation based on perovskites have made great progress and remarkable achievements. Then, there is still a long way to go to satisfy the application of all-optical computing and neuro network. Therefore, great efforts will be made to promote the rapid development of perovskites in photonic memristive devices to meet the exponential growth of data storage and processing as well as brain-inspired synaptic and artificial intelligence.

For a three-terminal transistor, in Feng's work, a vertical ITO transistor based on the sodium alginate (SA)-based biopolymer electrolyte surface is fabricated [150]. The device less than 10 nm breaks through the ultra-short channel technology for the first time, and can be used to simulate the pain-perceptual nociceptors and the sensitization-regulated nociceptors. Therefore, it has a non-negligible prospect in the bionic robot with the requirements of regulating pain threshold, pain perception, sensitization

Table 2: Overview of optical memristive devices based on perovskites

Group	Structure	Application	Ref.
Wang et al.	Si/SiO ₂ /CsPbBr ₃ QDs/PMMA ^a /pentacene/Au	Photon artificial synapse	[10]
Yang et al.	ITO ^b /SnO ₂ /CsPbCl ₃ /TAPC ^c /TAPC:MoO ₃ /MoO ₃ /Ag/MoO ₃	Dual-terminal photonic artificial synapses	[11]
Ham et al.	ITO/OHPd:CH3NH3Pbl3/Ag	Photon artificial synapse	[139]
Lin et al.	ITO/PEDOT:PSS ^e /organic-inorganic hybrid perovskite/Cu	Nonvolatile memory	[140]
Gong et al.	Si/SiO ₂ /CsPbBr ₃ QDs/Al ₂ O ₃ /pentacene/Au	Photoelectric programmable memristor	[141]
Yang et al.	ITO/PMMA/PQDsf:PMMA/PMMA/Ag	Nonvolatile memory	[74]
Cai et al.	Si/Pt/PEDOT:PSS/Cs ₄ PbBr ₄ /Au	Nonvolatile memory	[142]
Zhang et al.	ITO/PMMA/PMMA:CsPbBr ₃ NCs ^g /PMMA/Au	RRAM ^h	[143]

a: PMMA represents polymethyl methacrylate; b: ITO represents indium tin oxide; c: TAPC represents 4,4'-Cyclohexylidenebis[N,N-bis (4-methylphenyl)benzenamine]; d: OHP represents organo-lead halide perovskite; e: PEDOT:PSS represents poly(3,4ethylenedioxythiophene) polystyrene sulfonate; f: PQDs represent perovskite quantum dots; g: NCs represent nanocrystals; h: RRAM represents resistive random-access memory.

behavior, and so on. For example, the pain threshold can be adjusted by adjusting the length of the transistor channel (channel layer thickness).

Van der Waals heterostructures have so good interfacial charge transfer characteristics that they are able to solve the problem of insufficient light absorption of single semiconductor materials. Therefore, Cheng's team developed a novel photoelectrically modulated neuromorphic device based on an ion-coupling gate-tunable vertical OD-CsPbBr₃-QDs/2D-MoS₂ hybrid-dimensional van der Waals heterojunction architecture [151]. The Boolean logic operation of "AND" and "OR" is completed by adjusting the presynaptic stimulus. In addition to the simulation of typical synaptic functions (such as STDP and PPF), the device can also simulate dendritic structures in biological synapses and achieve dendritic integration behaviors. The appearance of such devices has made great contributions to the development of the intelligent cognitive system and photoelectric neural computing.

Similarly, Xie *et al.* fabricated OD-CsPbBr₃-QDs/2D-MoS₂ mixed-dimensional heterojunction transistors capable of simulating biological visual adaptation [152]. Different frequencies and intensities of photoelectric cooperative stimulation have a key impact on the adaptive precision, sensitivity, inactivation, and desensitization of the device. For photoelectric neural devices, the exploration of devices of this kind is of great significance to the construction of artificial vision system and the manufacture of bionic robots.

4 Conclusion and prospects

With the rapid development of perovskite materials in recent years, new development possibilities have been brought to many fields, and we are in the era of a new "perovskite boom." In order to discuss some current research and development directions of perovskites, this review introduces the preparation of perovskite materials and summarizes their optical and electrical properties. On this basis, we focused on the application and development of perovskites in various fields, for instance, optical communications, solar cells, and information encryption and decryption, especially in the field of photonic memristive devices and reviewed the recent results of research.

Although perovskite has made breakthroughs in multiple fields, there are still many new opportunities and challenges that researchers need to face and solve in the future. In view of the short life span, perovskite has high research value in future high-speed optical communications. VLC has attracted wide attention due to its many advantages such as high data transmission rate, good security, and no electromagnetic interference. The characteristics of short response time, good stability, and ease of manufacture make it more conducive to large-scale commercial applications. At present, MAPbI₃, LPQDs, and organic/inorganic hybrid perovskites are all popular development directions. As a new field of perovskite, information encryption and decryption has broad research prospects. It can not only improve the security of information but can also perform repeated encryption and decryption. Although perovskite materials are suggested as a potential strategy for information encoding and decoding, the shortcomings of insufficient color modes still restrict their development. Therefore, it is still a huge challenge to develop luminescent materials and systems with efficient encryption and decryption functions. At present, metal halide perovskite materials have attracted a lot of attention in many research fields. It is also a feasible idea to develop luminescent materials with excellent performances by changing the chemical composition or structure of the material. In addition, the outstanding characteristics of perovskite make it an attractive prospect in the novel and promising field of artificial intelligence. Advanced photon memristive devices based on perovskite materials have excellent resistance switching characteristics. Due to the unique signal transmission characteristics of the memristive devices and the excellent performance of the perovskite, the perovskite-based memristive devices can flexibly combine light and electricity, which will break the limitations of traditional electrical devices. It can also simulate the signal learning, processing, and memory of the nervous system, and at the same time will promote the development of artificial intelligence and make further progress in practical applications. However, equipment-level obstacles have always plagued researchers. For example, poor sustainability, non-linear writing, and excessive writing noise all limit the efficiency of the memristor close to the neural architecture. In practice, it also faces technical obstacles in synthesis, manufacturing, and assembly.

Overall, perovskite materials have quite optimistic application prospects and have proved to be promising candidates in many fields. We firmly believe that in the near future, with the advancement of device design, manufacturing, and materials, logic devices based on perovskite materials will become promising candidates for commercial applications, especially integrated chip fusing sensing, storage, and computing.

Funding information: This work was supported in part by the National Key Research and Development Program of China (2021YFE0105300), Key Technologies R&D Program of Huzhou City Science and Technology Project (2020GG03), Natural Science Foundation of Jiangsu Province (BK20220399), University Science Research Project of Jiangsu Province (20KJB510014), NJUPTSF (NY220078), National Natural Science Foundation of China (62204128, 61974031, and 61904087), National and Local Joint Engineering Laboratory of RF Integration and Micro-Assembly Technology (KFJJ20200203), Foundation of Jiangsu Provincial Double-Innovation Doctor Program (JSSCBS20210522).

Author contributions: All authors have accepted responsibility for the entire content of this manuscript and approved its submission.

Conflict of interest: The authors state no conflict of interest.

Data availability statement: All data generated or analyzed during this study are included in this published article.

References

- Liu MZ, Johnston MB, Snaith HJ. Efficient planar heterojunction perovskite solar cells by vapour deposition. Nature. 2013;501:395-8.
- [2] Sutherland BR, Sargent EH. Perovskite photonic sources. Nat Photonics. 2016;10(5):295–302.
- [3] Wang D, Wright M, Elumalai NK, Uddin A. Stability of perovskite solar cells. Sol Energy Mater Sol Cell. 2016;147:255-75.
- [4] Yang SD, Fu WF, Zhang ZQ, Chen HZ, Li CZ. Recent advances in perovskite solar cells: efficiency, stability and lead-free perovskite. J Mater Chem A. 2017;5:11462–82.
- [5] Hong, K, Van, Le, Kim, SY, Jang, HW. Low-dimensional halide perovskites: review and issues. J Mater Chem C. 2018;6:2189-209.
- [6] Zhang CY, Wang B, Li WB, Huang SQ, Kong L, Li ZC, et al. Conversion of invisible metal-organic frameworks to luminescent perovskite nanocrystals for confidential information encryption and decryption. Nat Commun. 2017;8:1–9.
- [7] Sun C, Su SJ, Gao ZY, Liu HX, Wu H, Shen XY, et al. Stimuliresponsive inks based on perovskite quantum dots for advanced full-color information encryption and decryption. ACS Appl Mater Interfaces. 2019;11:8210-6.
- [8] Pang PY, Jin GG, Liang C, Wang BZ, Xiang W, Zhang DL, et al. Rearranging low-dimensional phase distribution of quasi-2D perovskites for efficient sky-blue perovskite light-emitting diodes. ACS Nano. 2020;14:11420-30.
- [9] Xu LM, Li JH, Cai B, Song JZ, Zhang FJ, Fang T, et al. A bilateral interfacial passivation strategy promoting efficiency and stability of perovskite quantum dot light-emitting diodes. Nat Commun. 2020;11:1–12.
- [10] Wang Y, Lv ZY, Chen JR, Wang ZP, Zhou Y, Zhou L, et al. Photonic synapses based on inorganic perovskite quantum dots for neuromorphic computing. Adv Mater. 2018;30:1802883.
- [11] Yang L, Singh M, Shen SW, Chih KY, Liu SW, Wu CI, et al.

 Transparent and flexible inorganic perovskite photonic artificial synapses with dual-mode operation. Adv Funct Mater.
 2021;31:2008259.
- [12] Sun YL, Qian L, Xie D, Lin YX, Sun MX, Li WW, et al. Photoelectric synaptic plasticity realized by 2D perovskite. Adv Funct Mater. 2019;29:1902538.
- [13] Yin L, Huang W, Xiao RL, Peng WB, Zhu YY, Zhang YQ, et al. Optically stimulated synaptic devices based on the hybrid structure of silicon nanomembrane and perovskite. Nano Lett. 2020;20:3378–87.
- [14] Kojima A, Teshima K, Shirai Y, Miyasaka T. Organometal halide perovskites as visible-light sensitizers for photovoltaic cells. J Am Chem Soc. 2019;131:6050–1.
- [15] Wang ZP, Lin QQ, Wenger B, Christoforo MG, Lin YH, Kiug MT, et al. High irradiance performance of metal halide perovskites for concentrator photovoltaics. Nat Energy. 2018;3(10):855-61.
- Jeong M, Choi IW, Go EM, Cho Y, Kim M, Lee B, et al. Stable perovskite solar cells with efficiency exceeding 24.8% and 0.3-V voltage loss. Science. 2020;369(6511):1615-20.
- 17] Wu H, Zhang Y, Zhang XY, Lu M, Sun C, Bai X, et al. Fine-tuned multilayered transparent electrode for highly transparent

- perovskite light-emitting devices. Adv Electron Mater. 2018:4:1700285.
- [18] Li CL, Zang ZG, Chen WW, Hu ZP, Tang XS, Hu W, et al. Highly pure green light emission of perovskite CsPbBr₃ quantum dots and their application for green light-emitting diodes. Opt Express. 2016;24:15071-8.
- Zheng F, Yang BB, Cao PY, Qian XL, Zou J. A novel bulk phosphor for white LDs: CsPbBr₃/Cs₄PbBr₆ composite quantum dots-embedded borosilicate glass with high PLQY and excellent stability. J Alloy Compd. 2020;818:153307.
- [20] Liu RH, Zhang JQ, Zhou H, Song ZH, Song ZN, Grice CR, et al. Solution-processed high-quality cesium lead bromine perovskite photodetectors with high detectivity for application in visible light communication. Adv Opt Mater. 2020;8(8):1901735.
- Li SX, Xu YS, Li CL, Guo Q, Wang G, Xia H, et al. Perovskite [21] single-crystal microwire-array photodetectors with performance stability beyond 1 year. Adv Mater. 2020;32(28):2001998.
- [22] Liang SM, Lu Z, Ding XR, Li JX, Tang Y, Li ZT, et al. Perovskite liquid quantum dots as a color converter for LD-based white lighting system for visible light communication. 2019 16th China International Forum on Solid State Lighting & 2019 International Forum on Wide Bandgap semiconductors: SSLChina & IFWS 2019 Proceedings; 2019. p. 277-9.
- [23] Jiang K, Zhang L, Lu JF, Xu CX, Cai CZ, Lin HW, et al. Triplemode emission of carbon dots: applications for advanced anti-counterfeiting. Angew Chem. 2016;128:7347-51.
- Qin B, Chen HY, Liang H, Fu L, Liu XF, Qiu XH, et al. Reversible [24] photoswitchable fluorescence in thin films of inorganic nanoparticle and polyoxometalate assemblies. J Am Chem Soc. 2010;123:2886-8.
- [25] Sun HB, Liu SJ, Lin WP, Zhang KY, Lv W, Huang X, et al. Smart responsive phosphorescent materials for data recording and security protection. Nat Commun. 2014;5(1):1-9.
- [26] Liu F, Zhang YH, Ding C, Kobayashi S, Izuishi T, Nakazawa N, et al. Highly luminescent phase-stable CsPbI₃ perovskite quantum dots achieving near 100% absolute photoluminescence quantum yield. ACS Nano. 2017;11:10373-83.
- Koscher BA, Swabeck JK, Bronstein ND, Alivisatos AP. Essentially trap-free CsPbBr3 colloidal nanocrystals by postsynthetic thiocyanate surface treatment. J Am Chem Soc. 2017;139:6566-9.
- Wang Y, Li XM, Sreejith S, Cao F, Wang Z, Stuparu MC, et al. Photon driven transformation of cesium lead halide perovskites from few-monolayer nanoplatelets to bulk phase. Adv Mater. 2016;28:10637-43.
- [29] Pradhan B, Das S, Li JX, Chowdhury F, Cherusseri J, Pandey D, et al. Ultrasensitive and ultrathin phototransistors and photonic synapses using perovskite quantum dots grown from graphene lattice. Sci Adv. 2020;6(7):5225.
- [30] Niu YJ, He DC, Zhang ZG, Zhu J, Gavin T, Falaras P, et al. Improved crystallinity and self-healing effects in perovskite solar cells via functional incorporation of polyvinylpyrrolidone. J Energy Chem. 2022;68:12-8.
- Wang Y, Zhang ZM, Lan YJ, Song Q, Li MZ, Song YL. Tautomeric molecule acts as a "sunscreen" for metal halide perovskite solar cells. Angew Chem. 2021;133(16):8755-9.
- Hou JW, Chen P, Shukla A, Krajnc A, Wang TS, Li XM, et al. Liquid-phase sintering of lead halide perovskites and

- metal-organic framework glasses. Science. 2021;374(6567):621-5.
- [33] Li MJ, Li HY, Zhuang QX, He DM, Liu BB, Chen C, et al. Stabilizing perovskite precursor by synergy of functional groups for NiOx-based inverted solar cells with 23.5% efficiency. Angew Chem Int Ed. 2022;61(35):e202206914.
- Liu JY, Chen KQ, Khan SA, Shabbir B, Zhang YP, Khan Q, et al. Synthesis and optical applications of low dimensional metalhalide perovskites. Nanotechnology. 2020;31(15):152002.
- [35] Choi J, Han JS, Hong K, Kim SY, Jang HW. Organic-inorganic hybrid halide perovskites for memories, transistors, and artificial synapses. Adv Mater. 2018;30(42):1704002.
- [36] Wang Y, Lv ZY, Zhou L, Chen XL, Chen JR, Zhou Y, et al. Emerging perovskite materials for high density data storage and artificial synapses. J Mater Chem C. 2018;6(7):1600-17.
- [37] Zhao XN, Xu HY, Wang ZQ, Lin Y, Liu YC. Memristors with organic-inorganic halide perovskites. InfoMat. 2019;1(2):183-210.
- [38] Pecunia V, Occhipinti LG, Chakraborty A, Pan Y, Peng YH. Lead-free halide perovskite photovoltaics: challenges, open questions, and opportunities. APL Mater. 2020;8(10):100901.
- López-Domínguez P, Van, Driessche I. Colloidal oxide per-[39] ovskite nanocrystals: from synthesis to application. Chimia. 2021;75(5):376.
- [40] Chen G, Zhu YP, Chen HM, Hu ZW, Hung SF, Ma NN, et al. An amorphous nickel-iron-based electrocatalyst with unusual local structures for ultrafast oxygen evolution reaction. Adv Mater. 2019;31(28):1900883.
- [41] Torres M, Ricote J, Pardo L, Calzada ML. Nanosize ferroelectric PbTiO₃ structures onto substrates. Preparation by a novel bottom-up method and nanoscopic characterisation. Integr Ferroelectr. 2008;99(1):95-104.
- [42] Arul NS, Nithya VD. Revolution of Perovskite. 1st edn. Singapore: Springer; 2020.
- [43] Ke WJ, Stoumpos CC, Zhu MG, Mao LL, Spanopoulos I, Liu J, et al. Enhanced photovoltaic performance and stability with a new type of hollow 3D perovskite {en} FASnI3. Sci Adv. 2017;3:1701293.
- [44] Mu X, Zhang HY, Xu L, Xu YY, Peng H, Tang YY, et al. Ferroelectrochemistry. APL Mater. 2021;9(5):051112.
- [45] Zhang HY, Chen XG, Zhang ZX, Song XJ, Zhang T, Pan Q, et al. Methylphosphonium Tin bromide: A 3D perovskite molecular ferroelectric semiconductor. Adv Mater. 2020;32:2005213.
- Tang YY, Li PF, Liao WQ, Shi PP, You YM, Xiong RG. Multiaxial [46] molecular ferroelectric thin films bring light to practical applications. J Am Chem Soc. 2018;140(26):8051-9.
- [47] Körbel S, Marques MAL, Botti S. Stable hybrid organic-inorganic halide perovskites for photovoltaics from ab initio high-throughput calculations. J Mater Chem A. 2018;6(15):6463-75.
- [48] Ozório MS, Srikanth M, Besse R, Da Silva JLF. The role of the A-cations in the polymorphic stability and optoelectronic properties of lead-free ASnI_3 perovskites. Phys Chem Chem Phys. 2021;23(3):2286-97.
- [49] Wu DF, Zhou J, Kang W, An K, Yang JY, Zhou M, et al. Ultrastable lead-free CsAgCl₂ perovskite microcrystals for photocatalytic CO₂ reduction. J Phys Chem Lett. 2021;12:5110-4.
- [50] Cao Q, Li YJ, Zhang H, Yang JB, Han J, Xu T, et al. Efficient and stable inverted perovskite solar cells with very high fill

- factors via incorporation of star-shaped polymer. Sci Adv. 2021;7(28):0633.
- [51] Wang ZP, Lin QQ, Chmiel FP, Sakai N, Herz LM, Snaith HJ, et al. Efficient ambient-air-stable solar cells with 2D-3D heterostructured butylammonium-caesium-formamidinium lead halide perovskites. Nat Energy. 2017;2:1-10.
- Fan JD, Ma YP, Zhang CL, Liu C, Li WZ, Schropp REI, et al. Thermodynamically self-healing 1D-3D hybrid perovskite solar cells. Adv Energy Mater. 2018;8:1703421.
- Ha ST, Liu XF, Zhang Q, Giovanni D, Sum TC, Xiong QH, et al. Synthesis of organic-inorganic lead halide perovskite nanoplatelets: towards high-performance perovskite solar cells and optoelectronic devices. Adv Opt Mater. 2014;2:838-44.
- [54] Noel NK, Habisreutinger SN, Wenger B, Klug MT, Hörantner MT, Johnston MB, et al. A low viscosity, low boiling point, clean solvent system for the rapid crystallisation of highly specular perovskite films. Energy Env Sci. 2017;10:145-52.
- Zhang SS, Wu HS, Chen WT, Zhu HM, Xiong ZZ, Yang ZC, et al. Solvent engineering for efficient inverted perovskite solar cells based on inorganic CsPbI2Br light absorber. Mater Today Energy. 2018;8:125-33.
- Tong Y, Bladt E, Aygüler MF, Manzi A, Milowska KZ, [56] Hintermayr VA, et al. Highly luminescent cesium lead halide perovskite nanocrystals with tunable composition and thickness by ultrasonication. Angew Chem Int Ed. 2016;55:13887-92.
- Duan JL, Zhao YY, He BL, Tang QW. High-purity inorganic [57] perovskite films for solar cells with 9.72% efficiency. Angew Chem. 2018;130:3849-53.
- Li X, Dar MI, Yi CY, Luo JS, Tschumi M, Zakeeruddin SM, et al. Improved performance and stability of perovskite solar cells by crystal crosslinking with alkylphosphonic acid ω-ammonium chlorides. Nat Chem. 2015;7:703-11.
- [59] Meng XY, Lin JB, Liu X, He X, Wang Y, Noda T, et al. Highly stable and efficient FASnI3-based perovskite solar cells by introducing hydrogen bonding. Adv Mater. 2019;31:1903721.
- Le TH, Lee S, Jo H, Jeong G, Chang M, Yoon H. Morphologydependent ambient-condition growth of perovskite nanocrystals for enhanced stability in photoconversion device. J Phys Chem Lett. 2021;12:5631-8.
- Yang G, Ren ZW, Liu K, Qin MC, Deng WY, Zhang HK, et al. Stable and low-photovoltage-loss perovskite solar cells by multifunctional passivation. Nat Photonics. 2021;15:681-9.
- Yang Y, Peng HR, Liu C, Arain Z, Ding Y, Ma S, et al. Bifunctional additive engineering for high-performance perovskite solar cells with reduced trap density. J Mater Chem A. 2019:7:6450-8.
- [63] Chu ZM, Zhao Y, Ma F, Zhang CX, Deng HX, Gao F, et al. Large cation ethylammonium incorporated perovskite for efficient and spectra stable blue light-emitting diodes. Nat Commun. 2020;11:1-8.
- Yang XG, Ma LF, Yan DP. Facile synthesis of 1D organicinorganic perovskite micro-belts with high water stability for sensing and photonic applications. Chem Sci. 2019;10:4567-72.
- Hu Y, Florio F, Chen ZZ, Phelan WA, Siegler MA, Zhou Z, et al. A chiral switchable photovoltaic ferroelectric 1D perovskite. Sci Adv. 2020;6:4213.

- [66] Spanopoulos I, Hadar I, Ke WJ, Guo PJ, Sidhik S, Kepenekian M, et al. Water-stable 1D hybrid Tin (II) iodide emits broad light with 36% photoluminescence quantum efficiency. J Am Chem Soc. 2020;142(19):9028-38.
- [67] Chen Y, Chen GY, Zhou Z, Li XM, Ma PP, Li LT, et al. Amplifying surface energy difference toward anisotropic growth of allinorganic perovskite single-crystal wires for highly sensitive photodetector. Adv Funct Mater. 2021;3:2101966.
- [68] Chen J, Fu YP, Samad L, Dang LN, Zhao YZ, Shen SH, et al. Vapor-phase epitaxial growth of aligned nanowire networks of cesium lead halide perovskites (CsPbX3, X = Cl, Br, I). Nano Lett. 2017;17(1):460-6.
- [69] Hossain MK, dos Reis R, Qarony W, Tsang YH, Ho JC, Yu KM, et al. Mechanism of non-catalytic chemical vapor deposition growth of all-inorganic CsPbX₃ (X = Br, Cl) nanowires. J Mater Chem C. 2021;9(9):3229-38.
- [70] Wang ZY, Liu JY, Xu ZQ, Xue YZ, Jiang LC, Song JC, et al. Wavelength-tunable waveguides based on polycrystalline organic-inorganic perovskite microwires. Nanoscale. 2016;8(12):6258-64.
- [71] Shamsi J, Urban AS, Imran M, De Trizio L, Manna L. Metal halide perovskite nanocrystals: synthesis, post-synthesis modifications, and their optical properties. Chem Rev. 2019;119:3296-348.
- [72] Protesescu L, Yakunin S, Bodnarchuk MI, Krieg F, Caputo R, Hendon CH, et al. Nanocrystals of cesium lead halide perovskites (CsPb X_3 , X = Cl, Br, and I): novel optoelectronic materials showing bright emission with wide color gamut. Nano Lett. 2015;15:3692-6.
- Swarnkar A, Marshall AR, Sanehira EM, Chernomordik BD, [73] Moore DT, Christians JA, et al. Quantum dot-induced phase stabilization of α-CsPbI₃ perovskite for high-efficiency photovoltaics. Science. 2016;354:92-5.
- Yang KY, Li FS, Veeramalai CP, Guo TL. A facile synthesis of CH₃NH₃PbBr₃ perovskite quantum dots and their application in flexible nonvolatile memory. Appl Phys Lett. 2017;110:083102.
- Yang DX, Huo DX. Cation doping and strain engineering of [75] CsPbBr3-based perovskite light emitting diodes. I Mater Chem C. 2020;8(20):6640-53.
- Chen ZH, Mei SL, He HY, Wen ZQ, Cui ZJ, Yang BB, et al. Rapid [76] large-scale synthesis of highly emissive solid-state metal halide perovskite quantum dots across the full visible spectrum. Opt Laser Technol. 2021;143:107369.
- He HY, Mei SL, Chen ZH, Liu SY, Wen ZQ, Cui ZJ, et al. Thioacetamide-ligand-mediated synthesis of CsPbBr₃-CsPbBr3 homostructured nanocrystals with enhanced stability. J Mater Chem C. 2021;9(34):11349-57.
- [78] Huang H, Li YX, Tong Y, Yao EP, Feil MW, Richter AF, et al. Spontaneous crystallization of perovskite nanocrystals in nonpolar organic solvents: A versatile approach for their shape-controlled synthesis. Angew Chem Int Ed. 2019;58(46):16558-62.
- [79] Chiba T, Hayashi Y, Ebe H, Hoshi K, Sato J, Sato S, et al. Anion-exchange red perovskite quantum dots with ammonium iodine salts for highly efficient light-emitting devices. Nat Photonics. 2018;12:681-7.
- [80] Kim YH, Kim S, Kakekhani A, Park J, Park J, Lee YH, et al. Comprehensive defect suppression in perovskite

- nanocrystals for high-efficiency light-emitting diodes. Nat Photonics. 2021;15:148-55.
- [81] Bao Z, Luo JW, Wang YS, Hu TC, Tsai SY, Tsai YT, et al. Microfluidic synthesis of CsPbBr₃/Cs₄PbBr₆ nanocrystals for inkjet printing of mini-LEDs. Chem Eng J. 2021;426:130849.
- Zhang Q, Su R, Du WN, Liu XF, Zhao LY, Ha ST, et al. Advances in small perovskite-based lasers. Small Methods. 2017:1:1700163.
- [83] Wang CY, hang YK, Wang AF, Wang Q, Tang HY, Shen W, et al. Controlled synthesis of composition tunable formamidinium cesium double cation lead halide perovskite nanowires and nanosheets with improved stability. Chem Mater. 2017;29:2157-66.
- Liu JY, Xue YZ, Wang ZY, Xu ZQ, Zheng CX, Weber B, et al. Two-dimensional CH3NH3PbI3 perovskite: synthesis and optoelectronic application. ACS Nano. 2016;10:3536-42.
- Wei HT, Fang YJ, Mulligan P, Chuirazzi W, Fang HH, Wang CC, et al. Sensitive X-ray detectors made of methylammonium lead tribromide perovskite single crystals. Nat Photonics. 2016;10:333-9.
- [86] Yang TY, Gregori G, Pellet N, Grätzel M, Maier J. The significance of ion conduction in a hybrid organic-inorganic leadiodide-based perovskite photosensitizer. Angew Chem Int Ed. 2015;54:7905-10.
- Senocrate A, Moudrakovski I, Kim GY, Yang TY, Gregori G, Grätzel M, et al. The nature of ion conduction in methylammonium lead iodide: A multimethod approach. Angew Chem Int Ed. 2017;56:7755-9.
- Kim GY, Senocrate A, Yang TY, Gregori G, Grätzel M, Maier J. [88] Large tunable photoeffect on ion conduction in halide perovskites and implications for photodecomposition. Nat Mater. 2018;17:445-9.
- Zhao XY, Deng WW. Printing photovoltaics by electrospray. Opto-Electron Adv. 2020;3(6):190038.
- Pachori S, Agrawal R, Shukla A, Verma AS. First-principles calculations for fundamental and spectroscopic screening of hybrid perovskite (HC(NH₂)₂PbI₃) formamidinium lead iodide. Mater Chem Phys. 2022;287:126149.
- Pachori S, Agarwal R, Prakash B, Kumari S, Verma AS. Fundamental physical properties of nontoxic Tin-based formamidinium $FASnX_3$ (X = I, Br, Cl) hybrid halide perovskites: future opportunities in photovoltaic applications. Energy Technol. 2022;10(2):2100709.
- MonikaPachori, S, Kumari S, Verma AS. An emerging high performance photovoltaic device with mechanical stability constants of hybrid (HC(NH₂)₂PbI₃) perovskite. J Mater Sci Mater Electron. 2020;31(20):18004-17.
- [93] MonikaPachori, S, Agrawal R, Choudhary BL, Verma AS. An efficient and stable lead-free organic-inorganic tin iodide perovskite for photovoltaic device: Progress and challenges. Energy Rep. 2022;8:5753-63.
- Kim HS, Kim SK, Kim BJ, Shin KS, Gupta MK, Jung HS, et al. [94] Ferroelectric polarization in CH₃NH₃PbI₃ perovskite. J Phys Chem Lett. 2015;6(9):1729-35.
- [95] Jia ED, Wei D, Cui P, Ji J, Huang H, Jiang HR, et al. Efficiency enhancement with the ferroelectric coupling effect using P (VDF-TrFE) in CH₃NH₃PbI₃ solar cells. Adv Sci. 2019;6(16):1900252.
- Taya A, Kumar S, Hackett TA, Kashyap MK. Optical absorption and stability enhancement in mixed lead, tin, and germanium

- hybrid halide perovskites for photovoltaic applications. Vacuum. 2022;201:111106.
- [97] Beal RE, Slotcavage DJ, Leijtens T, Bowring AR, Belisle RA, Nguyen WH, et al. Cesium lead halide perovskites with improved stability for tandem solar cells. J Phys Chem Lett. 2016;7:746-51.
- [98] Liu CM, Zeng QS, Zhao Y, Yu Y, Yang MX, Gao H, et al. Surface ligands management for efficient CsPbBrl₂ perovskite nanocrystal solar cells. Sol RRL. 2020;4:2000102.
- [99] He J, Su J, Lin ZH, Ma J, Zhou L, Zhang SY, et al. Enhanced efficiency and stability of all-inorganic CsPbI2Br perovskite solar cells by organic and ionic mixed passivation. Adv Sci. 2021;8:2101367.
- [100] Li MH, Shao JY, Jiang Y, Qiu FZ, Wang S, Zhang JQ, et al. Electrical loss management by molecularly manipulating dopant-free poly (3-hexylthiophene) towards 16.93% CsPbl₂Br solar cells. Angew Chem. 2021;133:16524-9.
- [101] Wu X, Liu YZ, Qi F, Lin F, Fu HT, Jiang K, et al. Improved stability and efficiency of perovskite/organic tandem solar cells with an all-inorganic perovskite layer. J Mater Chem A. 2021;9:19778-87.
- [102] Yan CJ, Li ZZ, Sun Y, Zhao J, Huang XC, Yang JL, et al. Decreasing energy loss and optimizing band alignment for high performance CsPbI₃ solar cells through guanidine hydrobromide post-treatment. J Mater Chem A. 2020;8:10346-53.
- [103] Yu BC, Shi JJ, Tan S, Cui YQ, Zhao WY, Wu HJ, et al. Efficient (>20%) and stable all-inorganic cesium lead triiodide solar cell enabled by thiocyanate molten salts. Angew Chem Int Ed. 2021;60:13436-43.
- [104] Wu X, Ma JJ, Qin MC, Guo XL, Li YH, Qin ZT, et al. Control over light soaking effect in all-inorganic perovskite solar cells. Adv Funct Mater. 2021;31:2101287.
- [105] Shi LX, Wang J, Zhou L, Chen YL, Yan J, Dai CA, et al. Facile insitu preparation of MAPbBr₃@UiO-66 composites for information encryption and decryption. J Solid State Chem. 2020;282:121062.
- [106] Liu XF, Zou L, Yang C, Zhao WL, Li XY, Sun B, et al. Fluorescence lifetime-tunable water-resistant perovskite quantum dots for multidimensional encryption. ACS Appl Mater Interfaces. 2020;12:43073-82.
- [107] Wu Y, Li XM, Wei Y, Gu Y, Zeng HB. Perovskite photodetectors with both visible-infrared dual-mode response and supernarrowband characteristics towards photo-communication encryption application. Nanoscale. 2018;10:359-65.
- [108] Jovicic A, Li JY, Richardson T. Visible light communication: opportunities, challenges and the path to market. IEEE Commun Mag. 2013;51:26-32.
- [109] Tsonev D, Chun H, Rajbhandari S, McKendry JJ, Videv S, Gu E, et al. A 3-Gb/s single-LED OFDM-based wireless VLC link using a gallium nitride µLED. IEEE Photonics Techno Lett. 2014;26:637-40.
- Pathak PH, Feng XT, Hu PF, Mohapatra P. Visible light com-[110] munication, networking, and sensing: A survey, potential and challenges. IEEE Commun Sury Tutor. 2015;17:2047-77.
- Le Minh H, O'Brien D, Faulkner G, Zeng LB, Lee K, Jung D, et al. 100-Mb/s NRZ visible light communications using a postequalized white LED. IEEE Photonics Techno Lett. 2009;21:1063-5.

- [112] Ghassemlooy Z, Alves LN, Zvanovec S, Khalighi MA. Visible light communications: theory and applications. 1st edn. Boca Raton: CRC press; 2017.
- [113] Haigh PA, Bausi F, Ghassemlooy Z, Papakonstantinou I, Le Minh H, Fléchon C, et al. Visible light communications: real time 10 Mb/s link with a low bandwidth polymer light-emitting diode. Opt Express. 2014;22:2830-8.
- [114] Yoshino M, Haruyama S, Nakagawa M. High-accuracy positioning system using visible LED lights and image sensor. IEEE RWS. 2008;439–42.
- [115] Li ZT, Cao K, Li JS, Tang Y, Ding XR, Yu BH. Review of blue perovskite light emitting diodes with optimization strategies for perovskite film and device structure. Opto-Electron Adv. 2021;4(2):02200019.
- [116] Yan DD, Zhao SY, Zhang YB, Wang HX, Zang ZG. Highly efficient emission and high-CRI warm white light-emitting diodes from ligand-modified CsPbBr₃ quantum dots. Opto-Electron Adv. 2022;5(1):200075.
- [117] Yang XL, Zhang XW, Deng JX, Chu ZM, Jiang Q, Meng JH, et al. Efficient green light-emitting diodes based on quasitwo-dimensional composition and phase engineered perovskite with surface passivation. Nat Commun. 2018;9:1–8.
- [118] Lin KB, Xing J, Quan LN, de Arquer FPG, Gong XW, Lu JX, et al. Perovskite light-emitting diodes with external quantum efficiency exceeding 20 percent. Nature. 2018;562:245–8.
- [119] Vashishtha P, Ng M, Shivarudraiah SB, Halpert JE. High efficiency blue and green light-emitting diodes using Ruddlesden-Popper inorganic mixed halide perovskites with butylammonium interlayers. Chem Mater. 2018;31:83-9.
- [120] Mei SL, Liu XY, Zhang WL, Liu R, Zheng LR, Guo RQ, et al. High-bandwidth white-light system combining a micro-LED with perovskite quantum dots for visible light communication. ACS Appl Mater Interfaces. 2018;10(6):5641-8.
- [121] Leitão MF, Islim MS, Yin L, Viola S, Watson S, Kelly A, et al. MicroLED-pumped perovskite quantum dot color converter for visible light communications. 2017 IEEE Photonics Conference; 2017. p. 69–70.
- [122] Trofimov P, Pushkarev AP, Sinev IS, Fedorov VV, Bruyère S, Bolshakov A, et al. Perovskite-gallium phosphide platform for reconfigurable visible-light nanophotonic chip. ACS Nano. 2020;14:8126–34.
- [123] Huang B, Liu JX, Han ZY, Gu Y, Yu DJ, Xu XB, et al. High-performance perovskite dual-band photodetectors for potential applications in visible light communication. ACS Appl Mater Interfaces. 2020;12:48765-72.
- [124] Wang WB, Zhao DW, Zhang FJ, Li LD, Du MD, Wang CL, et al. Highly sensitive low-bandgap perovskite photodetectors with response from ultraviolet to the near-infrared region. Adv Funct Mater. 2017;27(42):1703953.
- [125] Miao JL, Zhang FJ. Recent progress on highly sensitive perovskite photodetectors. J Mater Chem C. 2019;7(7):1741-91.
- [126] Tong SC, Sun J, Wang CH, Huang YL, Zhang CJ, Shen JQ, et al. High-performance broadband perovskite photodetectors based on CH₃NH₃Pbl₃/C8BTBT heterojunction. Adv Electron Mater. 2017;3(7):1700058.
- [127] Zhou GG, Sun R, Xiao Y, Abbas G, Peng ZC. A high-performance flexible broadband photodetector based on

- graphene-PTAA-perovskite heterojunctions. Adv Electron Mater. 2021;7(3):2000522.
- [128] Ma ZZ, Zhang YT, Li TT, Tang X, Zhao HL, Li JH, et al. Highperformance self-powered perovskite photodetector for visible light communication. Appl Phys A. 2020;126:1–8.
- [129] Xiao XT, Tang HD, Zhang TQ, Chen W, Chen WL, Wu D, et al. Improving the modulation bandwidth of LED by CdSe/ZnS quantum dots for visible light communication. Opt Express. 2016;24:21577-86.
- [130] Ding N, Xu W, Zhou DL, Ji YN, Wang Y, Sun R, et al. Extremely efficient quantum-cutting Cr³⁺, Ce³⁺, Yb³⁺ tridoped perovskite quantum dots for highly enhancing the ultraviolet response of Silicon photodetectors with external quantum efficiency exceeding 70%. Nano Energy. 2020;78:105278.
- [131] Kang CH, Dursun I, Liu GY, Sinatra L, Sun XB, Kong MW, et al. High-speed colour-converting photodetector with all-inorganic CsPbBr₃ perovskite nanocrystals for ultraviolet light communication. Light Sci Appl. 2019;8:1–12.
- [132] Mo QH, Chen C, Cai WS, Zhao SY, Yan DD, Zang ZG, et al. Room temperature synthesis of stable zirconia-coated CsPbBr₃ nanocrystals for white light-emitting diodes and visible light communication. Laser Photonics Rev. 2021;15(10):2100278.
- [133] Hu W, Cong H, Huang W, Huang Y, Chen LJ, Pan AL, et al.

 Germanium/perovskite heterostructure for high-performance and broadband photodetector from visible to infrared telecommunication band. Light: Sci Appl. 2019;8:1–10.
- [134] Prucnal PR, Shastri BJ, Teich MC. Neuromorphic photonics. 1st edn. Boca Raton: CRC press; 2017.
- [135] Ferreira de Lima T, Shastri BJ, Tait AN, Nahmias MA, Prucnal PR. Progress in neuromorphic photonics. Nanophotonics. 2017;6(3):577–99.
- [136] Chua L. Memristor-the missing circuit element. IEEE Trans Circuit Theory. 1971;18:507-19.
- [137] Hickmott TW. Low-frequency negative resistance in thin anodic oxide films. J Appl Phys. 1962;33(9):2669–82.
- [138] Asamitsu A, Tomioka Y, Kuwahara H, Tokura Y. Current switching of resistive states in magnetoresistive manganites. Nature. 1997;388:50–2.
- [139] Ham S, Choi S, Cho H, Na SI, Wang G. Photonic organolead halide perovskite artificial synapse capable of accelerated learning at low power inspired by dopamine-facilitated synaptic activity. Adv Funct Mater. 2019;9:1806646.
- [140] Lin GM, Lin YW, Cui RL, Huang H, Guo XH, Li C, et al. An organic-inorganic hybrid perovskite logic gate for better computing. J Mater Chem C. 2015;3:10793–8.
- [141] Gong Y, Wang Y, Li RH, Yang JQ, Lv ZY, Xing XC, et al. Tailoring synaptic plasticity in a perovskite QD-based asymmetric memristor. J Mater Chem C. 2020;8:2985–92.
- [142] Cai HZ, Lao MM, Xu J, Chen YK, Zhong CJ, Lu SR, et al. All-inorganic perovskite Cs₄PbBr₆ thin films in optoelectronic resistive switching memory devices with a logic application. Ceram Int. 2019;45:5724–30.
- [143] Zhang XN, Yang HY, Jiang ZG, Zhang Y, Wu SX, Pan H, et al. Photoresponse of nonvolatile resistive memory device based on all-inorganic perovskite CsPbBr₃ nanocrystals. J Phys Appl Phys. 2019;52:125103.
- [144] Ge C, Liu CX, Zhou QL, Zhang QH, Du JY, Li JK, et al. A ferrite synaptic transistor with topotactic transformation. Adv Mater. 2019;31(19):1900379.

- [145] Subramanian Periyal S, Jagadeeswararao M, Ng SE, John RA, Mathews N. Halide perovskite quantum dots photosensitized-amorphous oxide transistors for multimodal synapses. Adv Mater Technol. 2020;5(11):2000514.
- [146] Duan HX, Liang LY, Wu ZD, Zhang HB, Huang L, Cao HT. IGZO/ CsPbBr₃-Nanoparticles/IGZO neuromorphic phototransistors and their optoelectronic coupling applications. ACS Appl Mater Inter. 2021;13(25):30165-73.
- [147] Hao DD, Zhang JY, Dai SL, Zhang JH, Huang J. Perovskite/ organic semiconductor-based photonic synaptic transistor for artificial visual system. ACS Appl Mater Interfaces. 2020;12(35):39487-95.
- [148] Ma FM, Zhu YB, Xu ZW, Liu YL, Zheng XJ, Ju SM, et al. Optoelectronic perovskite synapses for neuromorphic computing. Adv Funct Mater. 2020;30(11):1908901.
- [149] Cheng YC, Li HJW, Liu B, Jiang LY, Liu M, Huang H, et al. Vertical OD-perovskite/2D-MoS₂ van der Waals heterojunction phototransistor for emulating photoelectric-

- synergistically classical pavlovian conditioning and neural coding dynamics. Small. 2020;16(45):2005217.
- [150] Feng GD, Jiang J, Zhao YH, Wang ST, Liu B, Yin K, et al. A sub-10 nm vertical organic/inorganic hybrid transistor for painperceptual and sensitization-regulated nociceptor emulation. Adv Mater. 2020;32(6):1906171.
- [151] Cheng YC, Shan KX, Xu Y, Yang JL, He J, Jiang J. Hardware implementation of photoelectrically modulated dendritic arithmetic and spike-timing-dependent plasticity enabled by an ion-coupling gate-tunable vertical 0D-perovskite/2D-MoS₂ hybrid-dimensional van der Waals heterostructure. Nanoscale. 2020;12(42):21798-811.
- [152] Xie DD, Wei LB, Xie M, Jiang LY, Yang JL, He J, et al. Photoelectric visual adaptation based on OD-CsPbBr3quantum-dots/2D-MoS2 mixed-dimensional heterojunction transistor. Adv Funct Mater. 2021;31(14):2010655.